PALYNOLOGICAL ANALYSIS OF OCEAN DRILLING PROGRAM LEG 210 WELLSITE 1276: TRENDS SURROUNDING THE PALEOCENE–EOCENE THERMAL MAXIMUM

Camille Haddad

April 2017

Distribution License

DalSpace requires agreement to this non-exclusive distribution license before your item can appear on DalSpace.

NON-EXCLUSIVE DISTRIBUTION LICENSE

You (the author(s) or copyright owner) grant to Dalhousie University the non-exclusive right to reproduce and distribute your submission worldwide in any medium.

You agree that Dalhousie University may, without changing the content, reformat the submission for the purpose of preservation.

You also agree that Dalhousie University may keep more than one copy of this submission for purposes of security, back-up and preservation.

You agree that the submission is your original work, and that you have the right to grant the rights contained in this license. You also agree that your submission does not, to the best of your knowledge, infringe upon anyone's copyright.

If the submission contains material for which you do not hold copyright, you agree that you have obtained the unrestricted permission of the copyright owner to grant Dalhousie University the rights required by this license, and that such third-party owned material is clearly identified and acknowledged within the text or content of the submission.

If the submission is based upon work that has been sponsored or supported by an agency or organization other than Dalhousie University, you assert that you have fulfilled any right of review or other obligations required by such contract or agreement.

Dalhousie University will clearly identify your name(s) as the author(s) or owner(s) of the submission, and will not make any alteration to the content of the files that you have submitted.

If you have questions regarding this license please contact the repository manager at dalspace@dal.ca.

Grant the distribution license by signing and dating below.

_____ _____

Name of signatory Date

Abstract

Offshore Newfoundland reflects the Cretaceous and Cenozoic sediments deposited offshore eastern Newfoundland and the rift and post-rift history of the North Atlantic. Site 1276 of Leg 210 of the Offshore Drilling Program was drilled to study the rift and subsequent post-rift sedimentation of the Newfoundland–Iberia system. Key biostratigraphic ages and paleoenvironments for the Creteceous-Paleogene section in 1276 were originally based on nannofossil, foraminifera and palynomorphs, all of wich are microfossils. In this study, I have utilized dinoflaglellate cysts, tiny unicellular organisms. Dinoflagellates have distinctive morphological features, such as tabulation patterns and excystment openings (archeopyles), which allow them to be assigned to genera and species, which have restricted stratigraphic ranges. These ranges allow the sediments to be dated, and dinocyst assemblages, for example, show changes that allow the Paleocene-Eocene thermal maximum (PETM) to be recognized. This event saw a significant rise in global average temperatures. In the present study, three broad intervals can be identified through the dinocyst assemblages: Selandian to Thanetian, late Ypresian to middle Lutetian, and middle Lutetian to early Priabonian. Peridinioid/ gonyaulacoid (P-Cyst/G-cyst) ratios have yielded a distinctive trend indicating an outer-neritic paleoenvironment with oceanic influence followed by a mass influx of inner-neritic species induced by the Paleocene Eocene thermal maximum and possibly the mid Eocene Climatic Optimum. Evidence for reworking among dinocysts has been recorded throughout the section.

Key Words: Palynology, Paleogene, dinoflagellates, PETM, paleoenvironments, dinocysts

Table of Contents

Table of Figures

Table of Tables

Acknowledgements

I'd like to extend my sincerest thanks and appreciation to my supervisors Rob Fensome & Graham Williams for their commitment towards this research project and allowing me to learn and expand my knowledge in an entirely new field of Geoscience. I'd also like to thank the GSC Atlantic for allowing me access to their slides and equipment, and to the Ocean Drilling Program for use of the samples (via GSC).

[1.0 Introduction]

Palynomorphs are fossil pollen, spores, dinoflagellate cysts (dinocysts) and other organic-walled microfossils. Palynology is the study of palynomorphs. Throughout the Mesozoic and Cenozoic, dinocysts were deposited in marine sediments and preserved in sedimentary successions [Williams et al. 2009]. Through the analysis of dinocyst assemblages, ages and paleoenvironments can be determined to aid in understanding the geological past. This research project will involve a palynological analysis of Paleogene dinocyst assemblages from ODP Site 1276, cored off Newfoundland as apart of Leg 210, with the intent of finding the age of the strata cored, and the paleoenvironmental trends associated with the global warming event known as the Paleocene–Eocene thermal maximum (PETM). Although some reconnaissance palynological work has been done on Site 1276, the present analyses will refine the biostratigraphy of the Paleogene section.

Biostratigraphy remains generally the best way to apply dates to Phanerozoic sedimentary rocks, and dinocysts are one of the most useful microfossil groups in the Mesozoic–Cenozoic. They are commonly sensitive to environmental change, which can provide insight into past climates [Williams et al. 2009]. The Paleogene is widely regarded as an extremely dynamic time, including the PETM and the subsequent drop in temperature to an icehouse state during the later Eocene and Oligocene [Zachos et al. 2001]. Dinocyst assemblages can also be used to investigate dynamic sedimentation processes that may have taken place during the rift and post-rift time periods of the Newfoundland and Iberia system. Using first and last occurrences of species, much can be inferred from these tiny organisms about the calibration of ages through the section.

Since 1966 the fundamental basis of the Deep-Sea Drilling Project (DSDP) and its successors, the Ocean Drilling Program (ODP, of which Leg 210 was part) and the Integrated Ocean Drilling Program (IODP), has been to provide data to aid in the study of the sea floor and subsurface. The vessel used during the DSDP, the Glomar Challenger, was replaced by the JOIDES Resolution during ODP (1983–2003), which featured 110 expeditions from regions across the globe. Leg 210 was conducted in the summer of 2003 and provided the material from which this study is conducted. Today, the IODP builds on the success of the ODP by

drawing on scientists from around twenty-five nations, with programs to 2023 emphasizing forward-looking science with future projects and scientific studied having a focus with an emphasis on climate change.

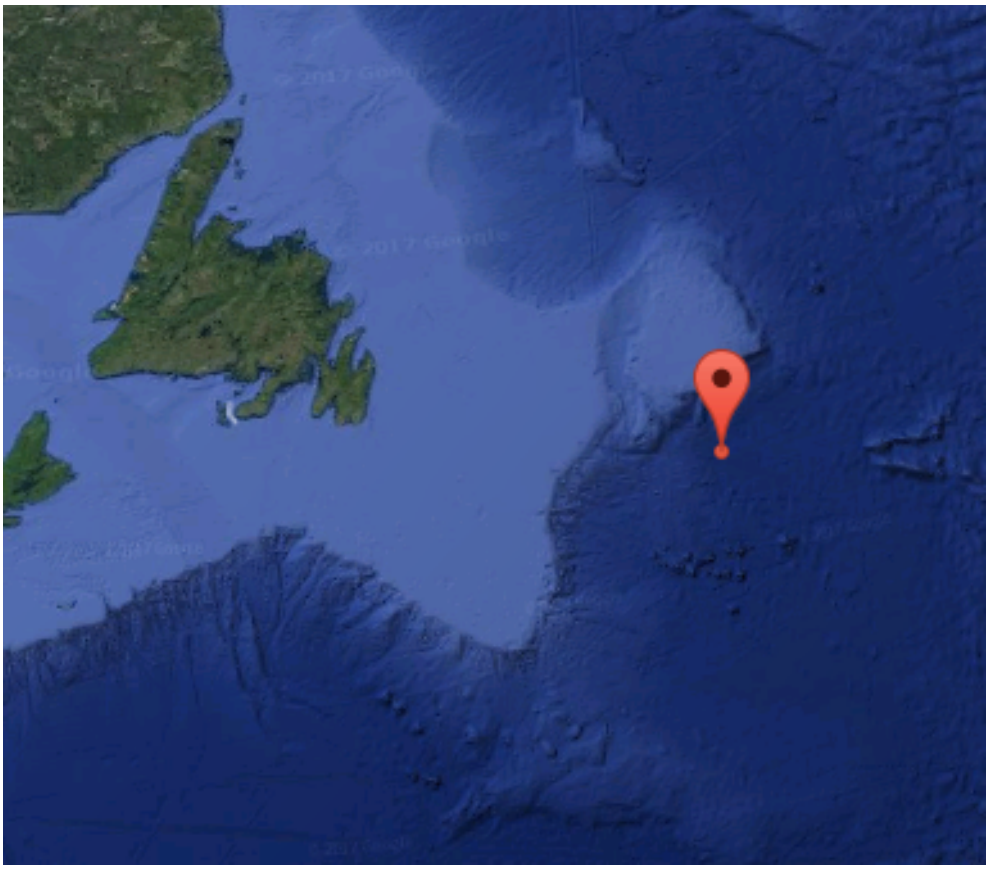

Figure 1.0 Satellite image showing location of well site 1276 of leg 210 [from Google Earth]

[2.0 Geological Setting]

[2.1 Regional Overview]

Site 1276, located on a deep-basin shelf beside Jean d' Arc basin off Newfoundland, and was drilled mainly as a scientific well as part of leg 210. All samples were extracted from a drill core through well 1276 (figure 2.0). Well 1276 is drilled along a deep basin shelf setting adjacent to the shallower areas of the Grand Banks and Flemish Cap. The well is one of two wells drilled in this proximal location. Comparison wells were drilled along the conjugate Iberian margin, as legs 149 and 173. The main focus of the study conducted by the Shipboard Scientific Party was to record the post-rift sedimentation of the Iberia-Newfoundland rift system, which is discussed further below. Paleoceanographic and biostratigraphic data can be analyzed through drill cores that have been extracted from the site. The drill core studied in the present work contains sediments spanning the late Cretaceous to early Oligocene interval, with good biotic recovery around the Paleocene–Eocene thermal maximum event [Tucholke et al. 2004]. As outlined in the site summary (Shipboard Scientific Party 2004), the total recovered core was approximately 790 m and consisted of interbedded mudstones and sandstones with the occurrence of limestone deposits, and constituted five subunits with distinctive lithological characteristics [Tucholke et al. 2004]. Today the site is on a passive margin, but it was part of a shallow rift basin throughout the Mesozoic. The deformational history of the basin can be divided into three phases of rifting and two stages of sedimentary infill.

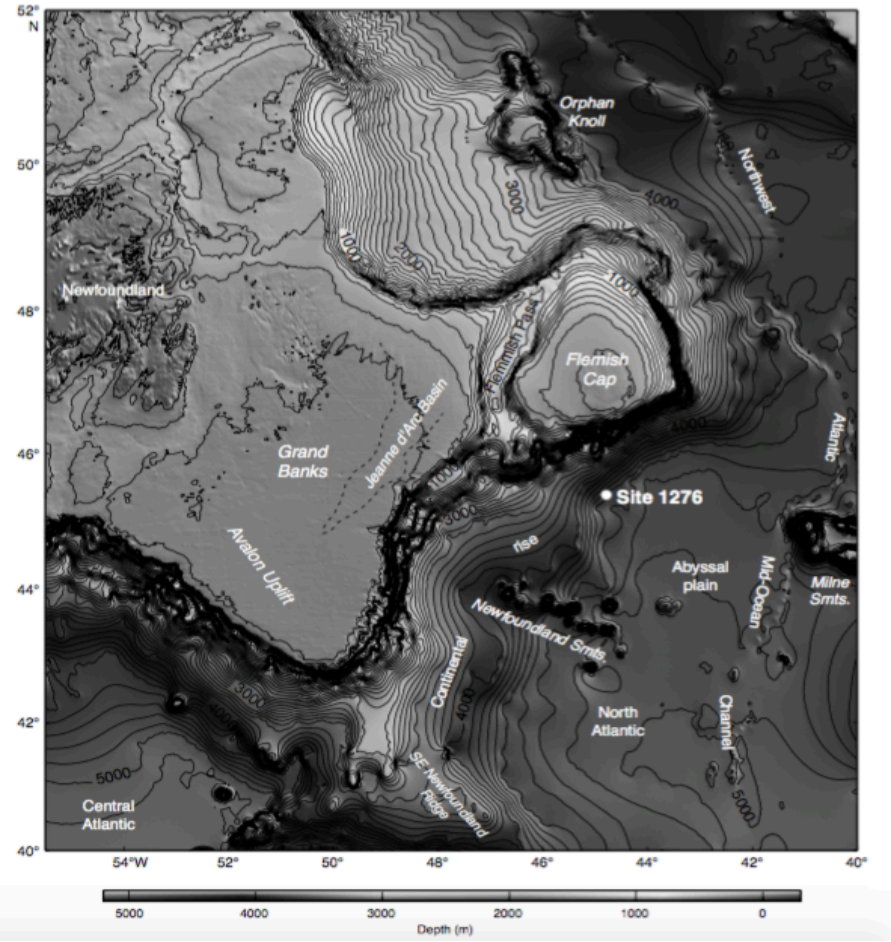

Figure 2.0 Depth elevation map showing location of Site 1276. Tucholke, B.E., Sibuet, J.-C., Klaus, A., et al., 2004

[2.2 Lithostratigraphy]

The core extracted at Site 1276 has been divided into five subunits based on lithological characteristics. Slides used in this study are from three of these subunits. The units reflect sedimentalogical, mineralogical and biogenic significance, as well as paleooceanographic conditions and diagenesis [Tucholke et al. 2004]. While not all units, or all parts of some units, are represented by my samples, a description of all units encompassing the Paleogene allows comparisons to be made between cyst assemblages and depositional history. It is important to note that slides 13R to 9R were missing from the material provided for this study (figure 2.1). This is most likely because most of the early to middle Eocene appeared to be barren of palynomorph assemblages [Tucholke et al. 2004], most likely due to the fact that it is within a

succession of turbidite and debris-flow deposits. This is inferred because sediments at Site 1276 were deposited at abyssal depths, an observation that aids in understanding the prominence of reworking throughout the succession [Tucholke et al. 2004]. This has implications when drawing conclusions. Slides analyzed include 16R to 14R and 8R to 6R inclusively. The initial site summary report (Shipboard Scientific Party 2004) made an attempt to correlate lithostratigraphic sections at Site 1276 with their Iberia counterparts. Furthermore, both Site 1276 and Iberian wells contain subunits that have been correlated with stratigraphic units in the North American Basin. The Plantagenet formation, of Late Cenomanian to Paleocene age, is identified at Site 1276 as well as at a few Iberian sites. The Plantagenet formation consists predominantly of pelagic and hemipalegic sediments, which are abundant throughout subunit three at Site 1276.

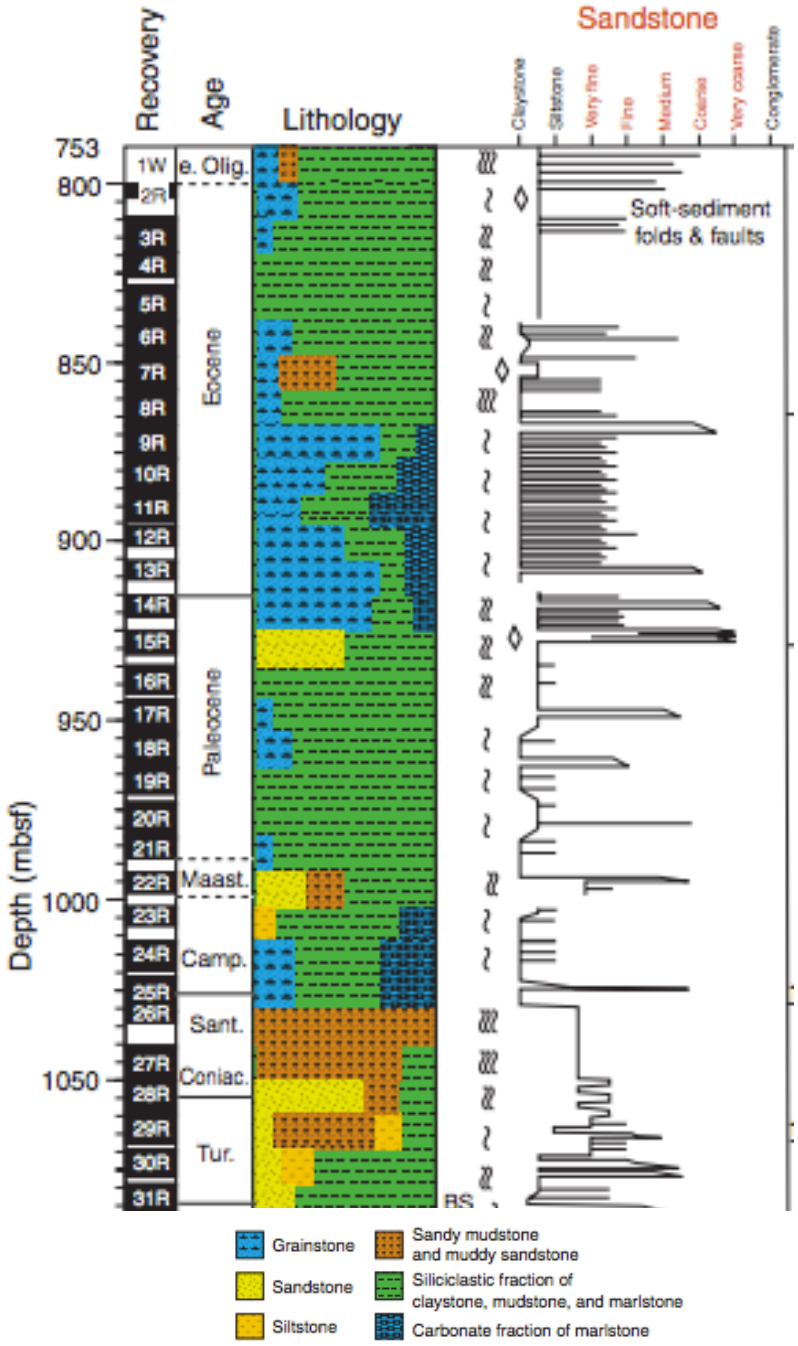

Figure 2.1 General stratigraphic column for Site 1276 as described by the Shipboard Scientific Party. Subunit 1 lies from 1W-14R, subunit 2 lies from 8R-14R and subunit 3 lies from 14R-24R. Ages are determined from previous nannofossil evidence in preliminary studies [From Tucholke et al. 2004].

[2.2.1 Subunit One]

This subunit has a top at approximately 753 m below sea floor (mbsf) and a bottom at 864.73 mbsf according to the Shipboard Scientific Party (2004), who reported that it ranges from the middle Eocene to the early Oligocene based on biostratigraphic data. They reported a hiatus between subunits one and two based on palynomorph and nannofossil evidence. This hiatus cannot be identified through the use of dinocysts because the appropriate slides are not in the set. Subunit one contains almost all the samples studied in this project. Subunit two, discussed in more detail below, was not represented by many productive samples. Unit one is described as a mudstone-dominated succession with interbedded muddy sandstones and some coarser sandy mudstones with larger mudstone clasts and minor reworked calcareous grainstone in thin graded beds with occasional rip-up clasts [Tucholke et al. 2004]. Drill cores also show that the laminated sandstone beds of subunit one contain mud-filled burrows, and cross-cutting turbiditic features, though the parallel laminated beds are mostly in the grainstones. Upslope debris flow deposits as well as rip-up clasts within sandy mudstones are also present throughout subunit one (figure 2.2).

Depositional features suggest that there was a significant amount of terrigenous influence on sediment deposition. Cuttings samples also show high variation in sediment deformation. Structural features include faulting, small scale folding and shear zones [Tucholke et al. 2004].

It is unclear whether diagenetic and deformational history within subunit one would have a significant impact on palynomorph preservation. Hemipelagic deposition was interrupted by gravity-flow and turbidite deposits incorporating upslope Cretaceous aged material. This indicates that a high level of reworking could affect palynomorph assemblages. Bioturbation could also have an impact on dinocyst assemblages.

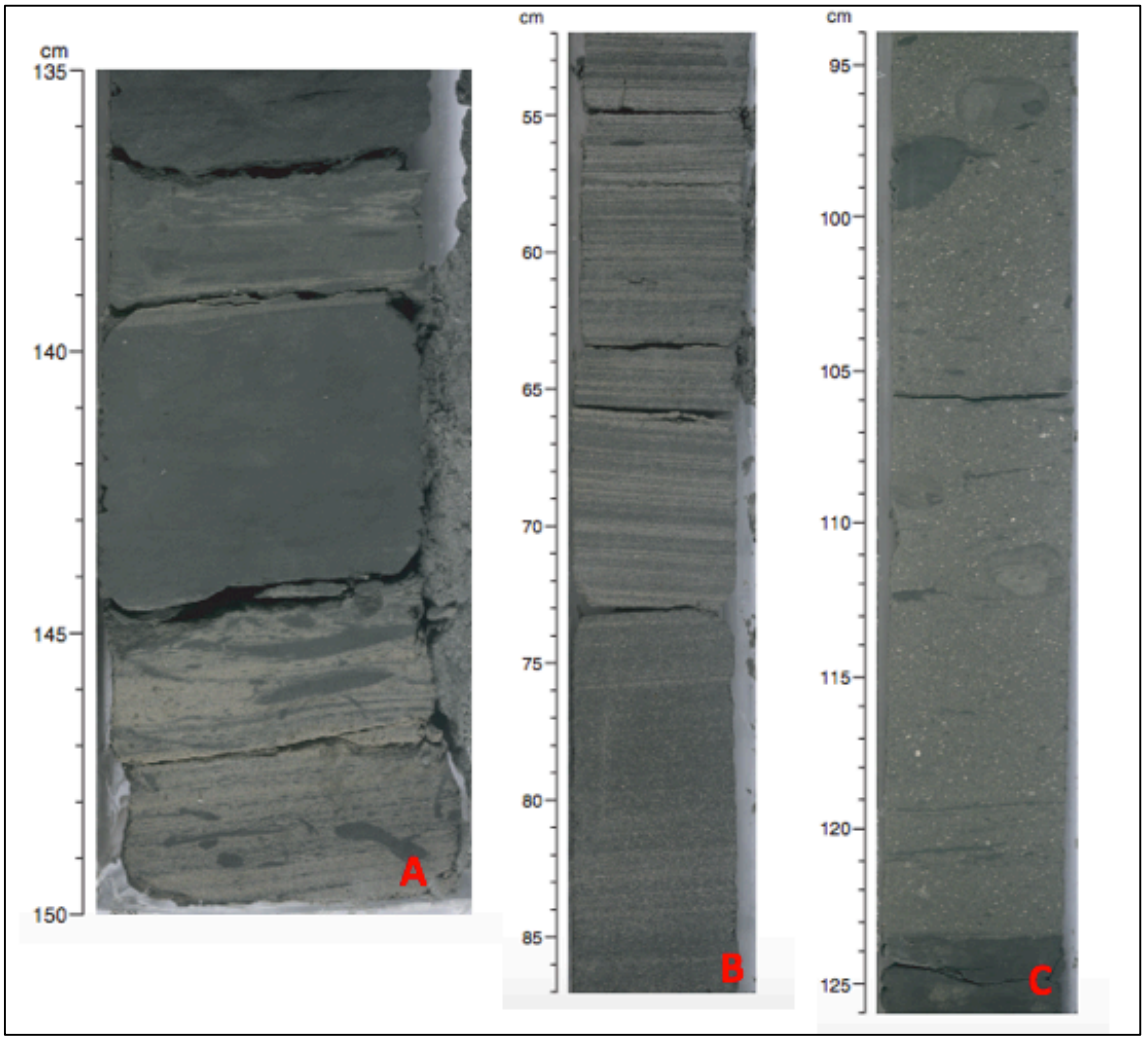

Figure 2.2 Core sections extracted from Site 1276, Leg 210. **A** - massive mudstone deposit with interlayed sands and mud rip-up clasts. **B**- Interbedded sandy mudstone laminations. **C**- Sandy mudstone deposits with large rounded mud rip-up clasts. [from Tucholke et al. 2004].

[2.2.2 Subunit Two]

Subunit two lies below subunit one, from 864.73 mbsf to 929.25 mbsp, with a hiatus in between as noted above. Compared with subunit one, subunit two contains significantly greater amounts of carbonate-rich lithologies [Tucholke et al. 2004]. The Shipboard Scientific Party (2004) reported that the age of this subunit as late Paleocene to middle Eocene. Palynomorphs were less abundant in this section, mostly due to higher input of debris flows and sediment deformation. Structural features such as minor faults are less prevalent in subunit

two than in subunit one, only visible through small-scale offsets and soft-sediment deformational features [Tucholke et al. 2004].

Subunit two is described as a grainstone- and calcareous-sandstone-dominated section, with interbedded dark-grey mudstone units that contrast with the lighter-coloured grainstone beds. The subunit also has dark-red to brownish marlstone units with grainstone laminations and biogenic traces at various intervals [Tucholke et al. 2004]. Grading is prominent in the grainstone units, with lower sections having medium to fine sand, changing to marlstone and calcareous mudstones in the higher part. The grainstones tend to be massive and homogenous towards the base of the unit, grading into finer sequences upwards and lamination near the top (figure 2.3 B). Sand intervals within the section also exhibit some cross-lamination, mostly at a small scale, but mudstone laminations are abundant throughout the section. The middle Eocene hiatus previously discussed occurs in subunit two (figure 2.3 C). This section features a light grey coarse grained deposit which marks the hiatus and was identified on the basis of biostratigraphy [Tucholke et al. 2004].

Subunit two is a distinct lithologic unit through the early Eocene, dominated by turbidite and low-density gravity deposits. Calcareous bioturbated claystones are interpreted as having been formed during times of slower deposition in which finer sediment settled. Subunit two has an abundance of sediments redeposited from upslope, notably late Cretaceous to Paleogene carbonate and silicic sediments. The base includes more silicic turbidites that are interpreted to be derived from Paleozoic igneous and metamorphic rocks on the continental margin [Tucholke et al. 2004]. Thus reworking potential is high in subunit two. The greater terrigenous component throughout subunit two likely reflects the warmer climates that dominated the Paleocene-Eocene transition. This higher terrigenous would result from increased weathering rates and sediment influx from coastal settings into neritic and shelfal margins. These factors would most probably have an effect on palynomorph assemblages through both the early Eocene hiatus and the less marked middle Eocene hiatus [Sluijs et al. 2004].

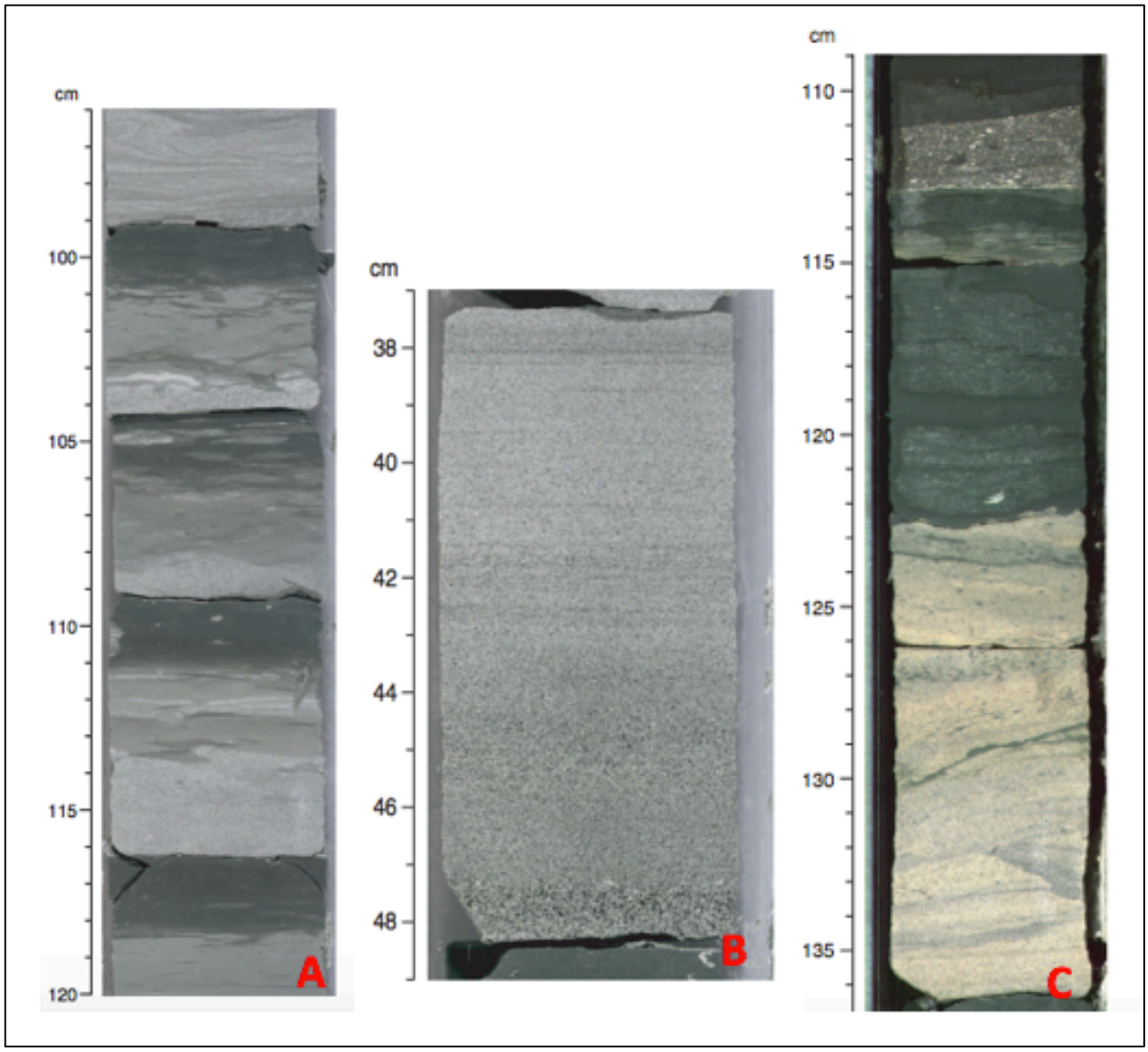

Figure 2.3 Core section extracted from Site 1276 along subunit 2. **A**- interbedded mudstone and calcareous grainstone deposits with some minor deformation. **B** - Fining upward grainstone deposit. **C** - Proposed site of the middle Eocene hiatus with a small grainstone dike present. [from Tucholke et al. 2004].

[2.2.3 Subunit Three]

Subunit three extends from 929.25 mbsf to 1028.00 mbsf. The Shipboard Scientific Party indicated its age as late Cretaceous to late Paleocene, but slides analyzed in this study represent only the Paleocene part of the section. Though reworking is possible as in the higher subunits, subunit three appears to have been deposited under quieter conditions, consisting

predominately of hemipalegic mudstones. Palynomorphs are indeed well preserved throughout this subunit, and within my samples encompassing almost all of the late Paleocene.

Subunit three is described as a mainly mudstone assemblage with minor grainstones and coarser calcareous sandstones making up the rest of the succession [Tucholke et al. 2004]. The mudstones are red to black and consist of well-graded gravity-flow deposits. High bioturbation rates throughout the succession suggest a slower sedimentation rate with the presence of kaolinite and smectite indicating a warm terrigenous source region [Tuchoke et al. 2004]. Reworked material occurs mostly near the top of the section and consists of poorly lithified granular carbonate clasts from upslope Cretaceous successions. The present study includes samples from all three subunits and extends from within the Paleocene to middle Eocene. In general, the section including samples 16R through 7R is a fining upward sequence (figure 2.4 B), with planar laminated to massive mudstones dominating the upper part of the succession [Tucholke et al. 2004]. Given the above criteria, preservation potential for palynomorphs is much higher in subunit three than in overlying units.

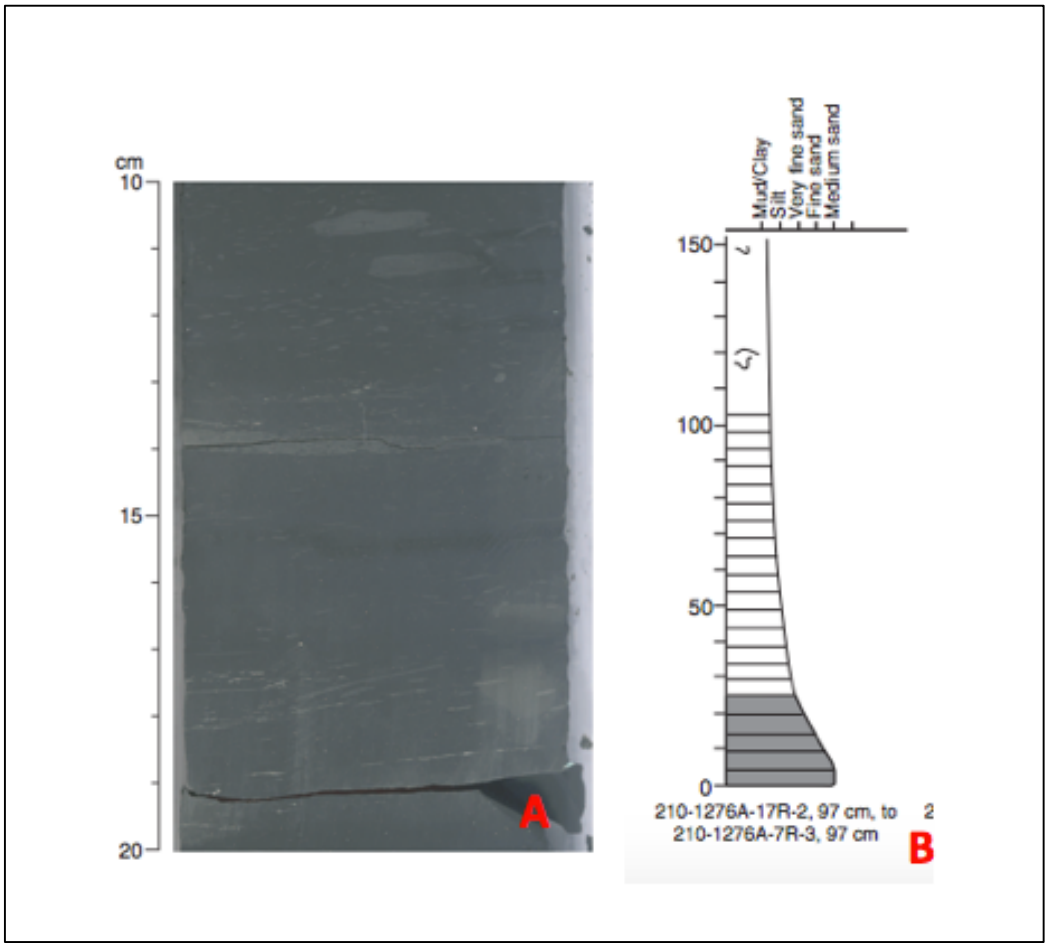

Figure 2.4 Core section extracted from site 1276, as a part of subunit 3. **A** - Massive fine grained mudstone deposit with minor rip-up clasts present. **B**- Generalized grain size stratigraphic column from the middle of subunit 3 to the beginning of subunit 1, demonstrating the fining upward sequence of the entire Paleogene succession.

[2.3 Tectonic History]

A passive margin today, offshore Newfoundland is characterized by shallow waters that cover the Grand Banks, dropping off into a deep-ocean setting where site 1276 is located. While the Paleogene featured little tectonic activity, both the post and syn-rift sediments at Site 1276 indicate a shift from a relatively anoxic to an oxygenated deep-basin setting. The conjugate Newfoundland-Iberia margins suggest a complex rift system that was active throughout the Mesozoic, with a late Triassic rift onset [Tucholke et al. 2007]. A second phase began in the middle Jurassic through the Cretaceous, consisting of three distinct episodes. Major rifting events culminated around the Albian, with subsequent post-rift deposition of fine-grained deposits throughout Paleocene [Tucholke et al. 2004].

Rifting began in the late Triassic to early Jurassic over a broad area on both the Grand Banks and Iberian margins [Tucholke et al. 2007]. The rift basins were subject to deposition of siliciclastic sediments throughout the Triassic and evaporate deposits during the Jurassic. The presence of widespread evaporate deposits in the Newfoundland-Iberian rift system and at the same time off southern African was because open ocean basins did not occur right away. As the rifting progressed into the middle Jurassic, the Grand Banks region began to subside, followed by syn-rift deposition of thick carbonate sequences [Tucholke & Sibuet 2007].

The second phase of rifting, with three distinct episodes, began in the middle Jurassic, with more intense seafloor spreading occurring in the earliest Cretaceous. Tucholke et al. (2007) concluded that the first rifting episode began in the middle Jurassic and extended into the early Cretaceous, the second occurred throughout the early Cretaceous, and the third spanned the middle Cretaceous. According to the Shipboard Scientific Party, these rifting episodes have little or no associated magmatic activity. Almost all rifting associated with the Newfoundland-Iberian system occurred from Triassic to early Cretaceous. The final rifting episode, during the Aptian, features dark mudstones with interbedded debris flow deposits, followed by deposition of Albian laminated mudstones with minor burrowing [Sibuet, Ryan et al. 1979]. Tucholke et al. (2007) noted that the sudden shift from mass-flow deposits to laminated mudstones indicates a more relaxed setting following the final rifting stage.

Post-rift sedimentation from Aptian to the late Paleocene features dark mudstone and claystone deposits with marly intervals throughout the succession [Tucholke & Sibuet 2007]. This succession is indicative of a deep-ocean setting that underwent significant post-rift sedimentation under relaxed anoxic conditions, before shifting to a well-oxygenated basin in the late Cretaceous. The Paleocene sediments accumulated under conditions that were not influenced by terrigenous deposits from the adjacent Grand Banks [Tucholke & Sibuet 2007]. However, well into the Paleocene there was a shift to more terrigenous deposition, indicating a shift in climate (i.e PETM). A drastic increase in climate would result in higher weathering rates within terrestrial regions resulting in higher sediment (i.e. hemipelagic sediments) influx to offshore environments.

[3.0 Background]

[3.1 Dinoflagellates]

Dinoflagellates are mostly single-celled eukaryotic organisms, the cell having two distinctive flagella that propel the organism forward in a “whirling motion” [Fensome e. al. 1993]. As well as the distinctive flagella, dinoflagellates are distinguished from similar organisms by possession of a special type of nucleus called a dinokaryon. A dinokaryon differs in that during mitosis (cell division) the chromosomes remain condensed [Williams et al. 2009]. Dinoflagellates are planktonic organisms that can be either autotrophic or heterotrophic, or both. Autotrophic dinoflagellates are photosynthetic and feed like plants, whereas heterotrophic forms lack (active) chloroplasts and ingest food like animals [Williams et al. 2009]. Motile cells may contain a protective armor-like cellulosic wall called a theca, which is divided up into separate thecal plates (figure 7 left). Dinoflagellates possessing a theca are termed thecate, whereas those that lack a theca are referred to as athecate [Fensome et al. 1993]. Under particular conditions some dinoflagellates produce outer shells formed from cyst walls known as dinocysts. There are resting, temporary and vegetative cysts; the walls of resting cysts can be formed of a very resistant organic material, and such cysts are preserved in the fossil record [Williams et al. 2009].

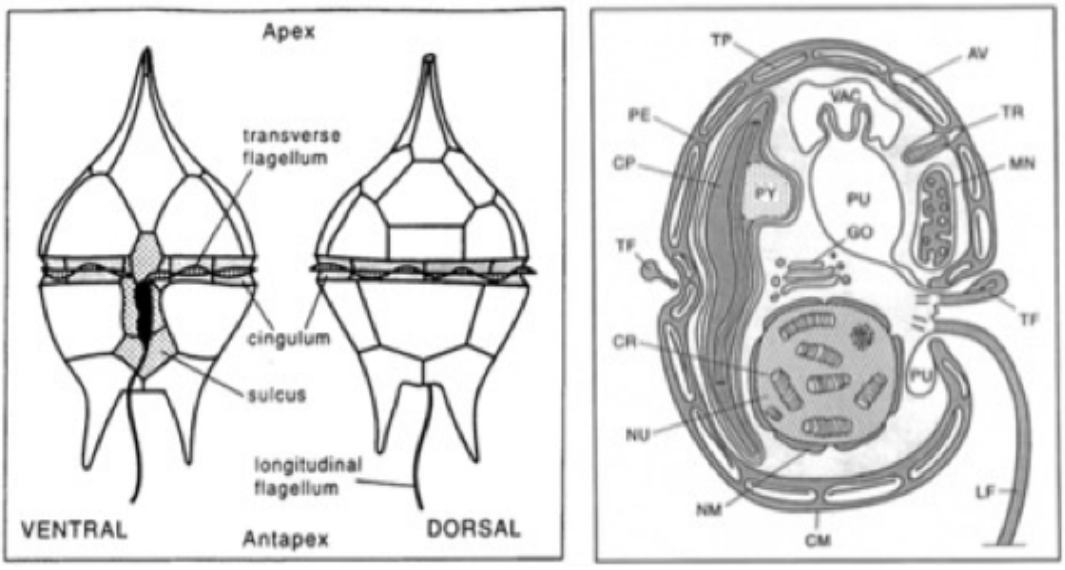

Figure 3.1 **Left** - General morphology of a motile cell (thecate), showing both the ventral and dorsal views. **Right** - cross section through a motile cell showing the biological makeup and important organelles. [from Williams et al. 2009].

Extant dinoflagellates show great morphological diversity, and the same is true for fossilized dinocysts. The thecal plates occur in patterns known as tabulation types, which are critical in classification, especially at generic and higher ranks. Although cysts do not have a theca with separable plates, tabulation is reflected in cysts in various ways, as explained below. Tabulation patterns can be one of six variations: gymnodinioid, dinophysioid, nannoceratopsioid, gonyaulacoid-peridinioid, suessioid and prorocentroid [Williams et al. 2009]. The gonyaulacoid-peridinioid tabulation pattern characterizes the vast majority of fossil dinocysts (figure 3.1 left). The gonyaulacoid–peridinioid tabulation is distinguished by thecal plates arranged a latitudinal and longitudinal series [Williams et al. 2009]. The tabulation notation system used mostly today was proposed by Kofoid (1907, 1909). In Kofoid`s terminology, thecal plates are related to `landmarks` on the cyst; these are the apex (anterior end), antapex (posterior end), the cingulum (an equatorial furrow) and the sulcus (a vertical furrow from which a longitudinal flagellum arises). Thus thecal plates that contact the apex are termed apical, plates in the cingulum are termed cingular and plates at the antapex are termed antapical. Plates which lie immediately anterior to, and those that lie immediately posterior to and the cingulum are known as postcingular and precingular plates respectively. Plates which lie between the precingular and apical series are known as anterior intercalary plates, whereas those located between the postcingular and antapical series are referred to as posterior intercalary [Williams et al. 2009]. Plates in different series are assigned symbols: apical (‘), precingular (‘’), cingular (c), postcingular (‘’’), antapical (‘’’’), sulcal (s), anterior intercalary (a) and posterior intercalary (p) [Williams et al. 2009]. Furthermore, plates can be assigned numbers which can then constitute a tabulation formula. The gonyaulacoid–peridinioid tabulation type features two distinct morphological cyst types constituting the orders Peridinales and Gonyaulacales (peridinioid and gonyaulacoid respectively), which can be divided further into suborders and families distinguished by details of tabulation [Fensome et al. 1996] (figure 3.2 right).

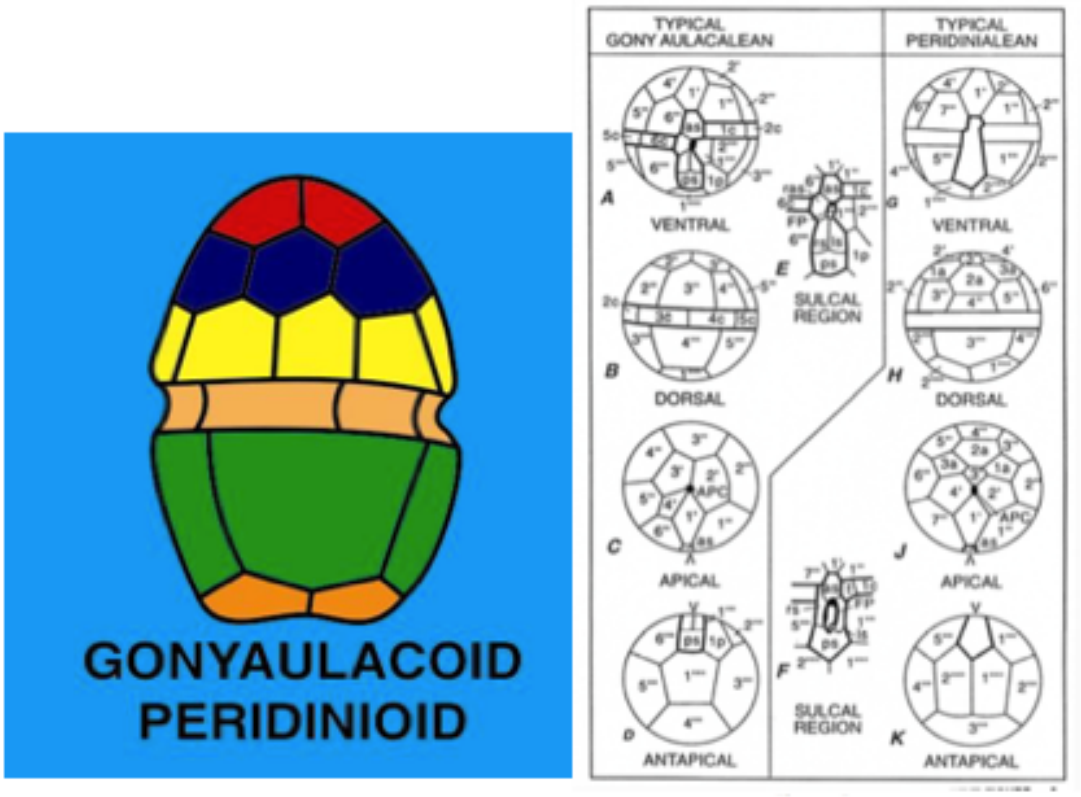

Figure 3.2 **Left** - Typical Gonyaulacoid-Peridinioid tabulation pattern**. Right** - Comparison between gonyaulacalean and peridinialean tabulation schemes proposed by Kofoid (1907, 1909). *Red – Apical plates, blue – precingular. tan – cingular, green – postcingular, orange – antapical.* The number and arrangement of the processes commonly reflect the number and arrangement of the plates. [from Williams et al. 2009] and [From R.A. Fensome, unpublished diagram and Williams et al. 2009].

Tabulation patterns of dinoflagellates are extremely important when identifying genera, but for species more detailed features, such as surface ornament or process type, are used. Cysts can be proximate or chorate. Proximate cysts are those that resemble the parent motile cell in overall shape. Chorate cysts have extensions, or processes, coming out from a usually spheroidal or ovoidal central body; the arrangement of the processes commonly reflect the arrangement of plates of the thecate stage. Cysts which show an intermediate morphology between chorate and proximate are known as proximochorate. [Williams et al. 2009].

Cysts which have two or more walls with spaces between them are known as cavate whereas cysts that show no separated wall layers are acavate [Williams et al. 2009]. The differences between these two cyst types can be seen in figure 9. The vast majority of

gonyaulacoid cysts tend to have apical or precingular archeopyles whereas one or more intercalary plate is always involved in the peridinioid archeopyle.

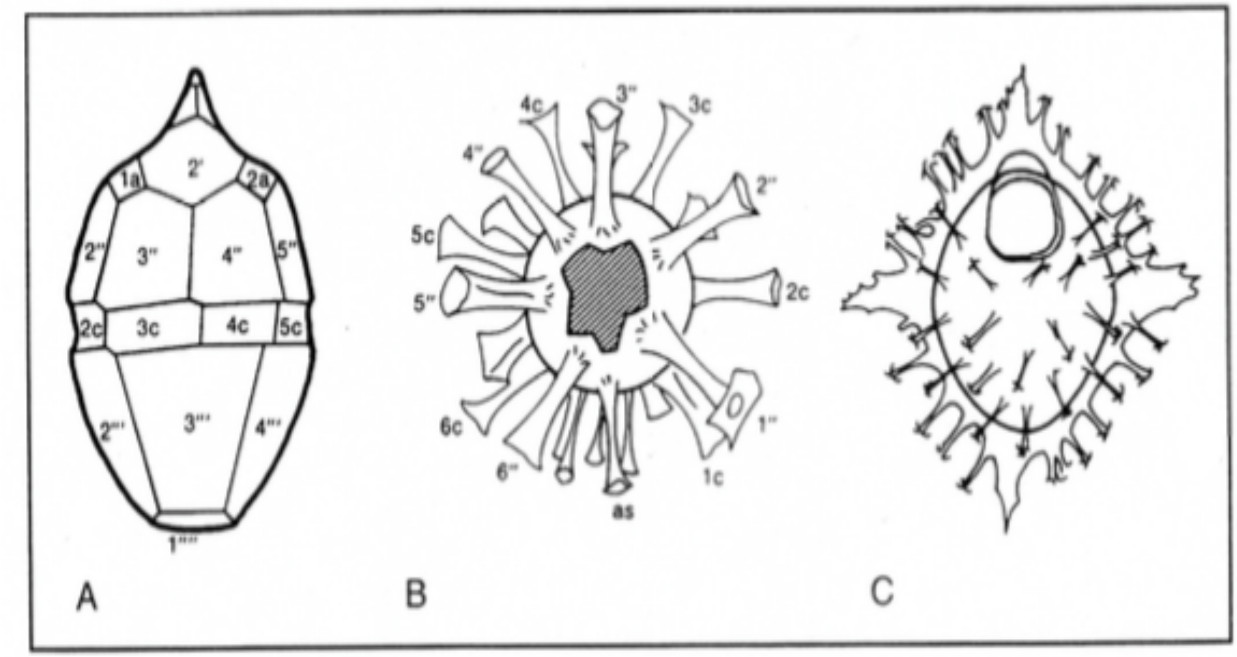

Figure 3.3 Difference between a proximate, chorate and proximochorate cyst. **A**- chorate acavate cyst. **B**- chorate acavate cyst. **C**- proximochorate acavate cyst. Shaded area represents the archeopyle [from Willaims et al. 2009].

Another very important feature is the archeopyle, or excystment opening. Evitt (1961) defined the archeopyle as an excystment site which reflects the plates on the cyst before deposition. Excystment involving loss of apical plates results in an apical archeopyle. Precingular archeopyles involve the loss of one or more precingular plates. Similarly, intercalary archeopyles result from the loss of intercalary plates [Evitt, 1961]. Archeopyles may form a flap like opening, but normally involve the removal of plates, and almost always occur on the epicyst. In some cases, archeopyles may be combined to form a larger opening [Williams et al. 2009]. The archeopyle is very important in defining genera.

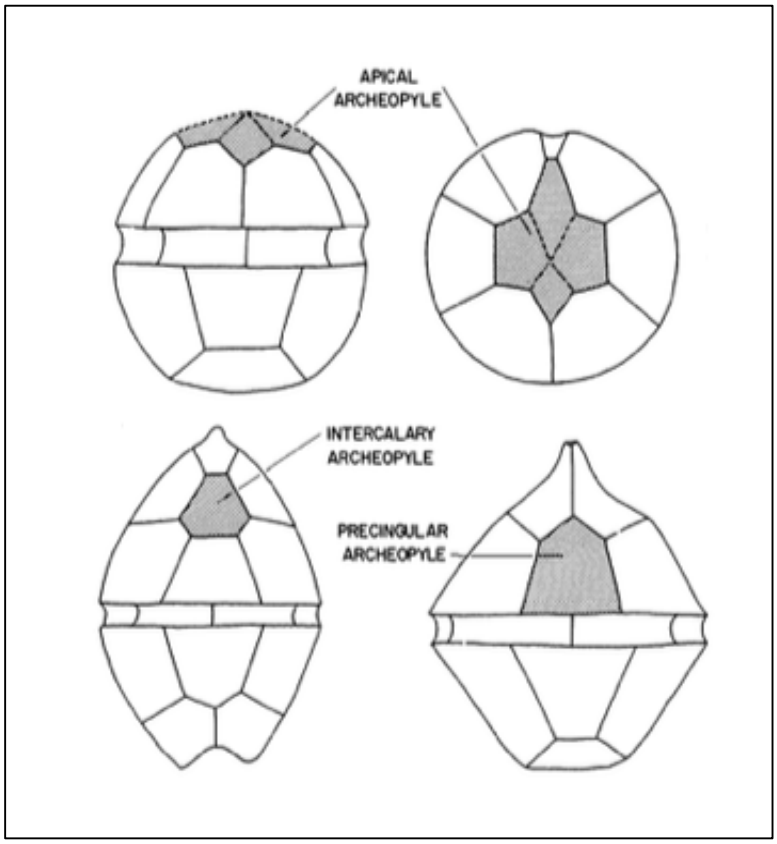

Figure 3.4 Graphic showing the various types of archeopyles produced by cyst forming dinoflagellates.[from Evitt 1961].

Biological makeup of dinoflagellates has a large role in how they interact with the environment around them and respond to change. Although modern dinoflagellates occupy marine and non-marine environments, most fossil dinocysts are marine. Dinoflagellates are sensitive to environmental change, such as salinity, which is evident from extant species. Particular genera tend to occupy different environmental settings, such as coastal, neritic and oceanic. [Williams et al. 2009]. Distance from shore plays an important role in the study of both extant and fossil dinoflagellates. Many dinoflagellates prefer neritic shelfal environments, with a select few favoring oceanic environments [Williams et al. 2009].

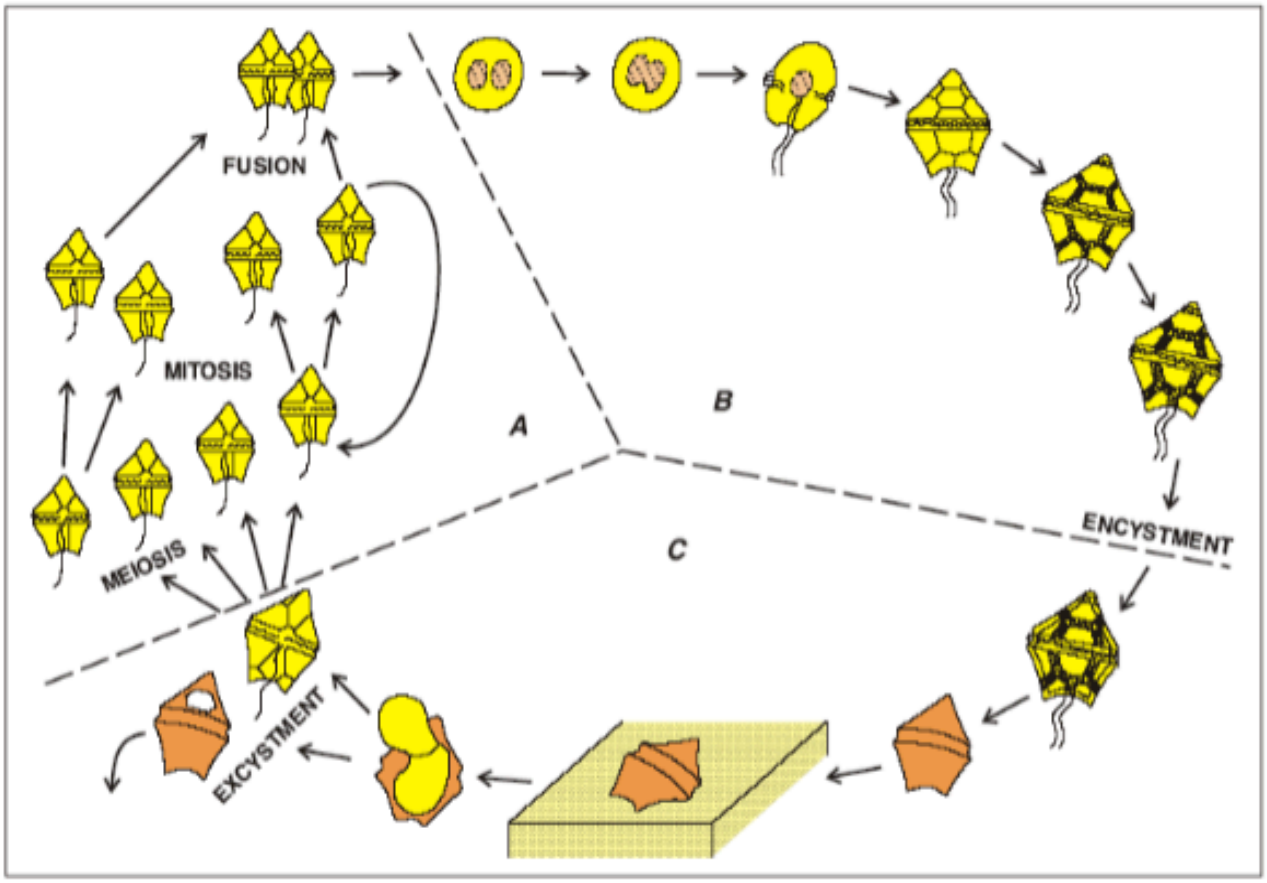

Figure 3.5 General lifecyle of a dinoflagellate showing cyst formation in **section C.** [from Williams et al. (2009), modified from Evitt (1985)].

[3.2 Paleocene-Eocene Thermal Maximum]

The geological record shows that the Paleogene was a climatically active time in Earth's history. Taxonomic variation in palynomorph assemblages reflects paleoenvironmental trends associated with climatic changes. The Paleocene-Eocene thermal maximum (PETM) is defined by a rapid rise in global average temperatures of almost five degrees within 10,000 years. This hyperthermal event is seen mainly through the rapid decrease in $^{13}C/^{12}C$ ratios and a drop in carbonates within the sedimentary record. Sea-surface temperatures are thought to have increased by almost eight degrees, as shown by the isotope records [Zachos et al. 2008]. Although the PETM is the main Paleogene climatic event, other important events are the early Eocene climatic optimum and the mid Eocene optimum (figure 3.6).

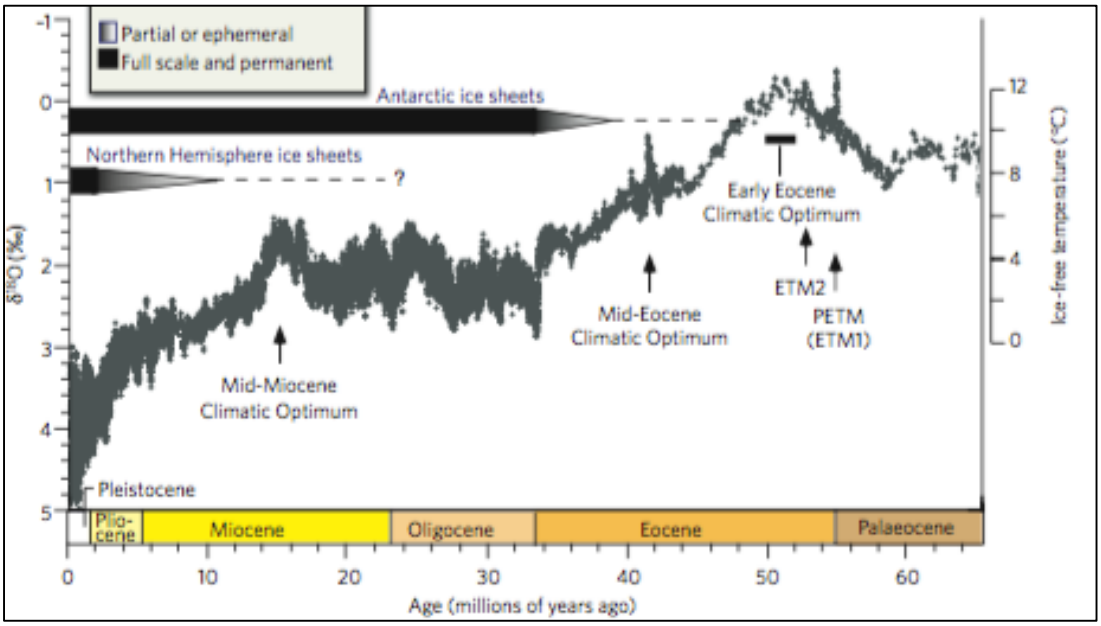

Figure 3.6 Graph showing the climatic dynamics of the Paleogene into the Miocene based on records from Deep Sea Ocean Drilling Project and Ocean Drilling Program stacked against ^{18}O percentage (‰, parts per thousand) showing ice free temperature. Temperature spikes can be seen throughout the Paleocene at PETM, ETM and Mid-Eocene Climatic Optimum. ETM1 & ETM2 signify two early Eocene climatic optimums [from Zachos et al. 2008].

From a palynological perspective the PETM had a global effect on dinoflagellate populations. Sluijs (2005) used the concept of productivity when looking at trends revolving around dinoflagellate populations through the Mesozoic and Paleogene. Productivity revolves around current patterns, upwelling systems and global wind patterns, which had a direct effect on dinoflagellate populations. Distinguishing between P-Cyst and G-Cyst within a succession and comparing them using a ratio can provide some insight into which environmental regime specific assemblages occupied [Sluijs et al. 2005]. This technique proves to be somewhat viable, especially when considering global spikes in P-Cyst abundances through the early Eocene. These localized spikes in P-Cyst assemblages can most likely be attributed to the slow recovery following the PETM, though P-Cyst seems to correlate heavily with sea surface temperature records through the Eocene [Sluijs et al. 2005]. Another primary impact of climate change at the PETM on dinoflagellate populations is the spike in the genus *Apectodinium*, which is a dinocyst with distinctive peridinioid dinocyst. This spike is evidence of the impact that warmer conditions had on marine plankton [Crouch et al. 2001]. Throughout the Paleogene an

increase in coastal productivity may be associated with certain assemblages and their relative abundances [Pross & Brinkhuis, 2005]. These abundances are especially important when considering outer neritic and oceanic environments. Various techniques have been applied to numerous palynological studies which use assemblage ratios in order to discern between paleoenvironments. Higher climatic conditions resulting in increased ocean surface temperatures would show a larger prevalence of inner neritic species associated with potentially higher terrigenous influence, or wind driven processes [Nohr-Hansen et al. 2016].

[4.0 Methodology]

As organic-walled microfossils, palynomorphs need to be extracted from sediment or rock. The general procedure is outlined in Barss & Williams (1973). After the sample has been crushed, 10% of hydrochloric acid is added to remove any carbonates. The residue is then washed and hydrofluoric acid is added (in a fume hood under controlled conditions) in order to remove any silicates. Hydrochloric acid is then again added after washing of the sample to remove any fluorides. Following washing and subsequent decanting, an oxidizing agent such as nitric acid or “Schulze” solution is added to oxidize unwanted organic material; this must be done with great care as over-oxidation can destroy the fossils. The residue is washed again and sieved, which concentrates any palynomorphs present. Most residues are stained with either red or brown dye. (Figure 13) shows the processing technique in more detail [Nohr-Hansen et al. 2016].

Slides provided by Geological Survey of Canada were analyzed at the Bedford Institute of Oceanography using a Nikon DS-Fi2 microscope. Other equipment used included a mounted Nikon Digital Sight DS-U3 camera used for taking images and a software program called NIS Elements for capturing, analyzing and editing images of dinocysts. Almost all dinoflagellates were viewed under the 40X lens and enhanced using a fine magnification. To conduct my analysis, I scanned each slide systematically, capturing every dinocyst photographically on the NIS Elements software. I would then digitally crop and add scales to each picture, and sorted the images into folders based on genera and eventually species. Where species could not be identified I simply left it in the genus folder. Slides were marked with series numbers corresponding to where they were extracted within the drill core. The series of slides which I analyzed are labelled 16R to 6R, although some slides are missing, reported barren by the ODP Shipboard Scientific Party. I did collect dinocyst data for the purpose of plots from other slides but did not capture assemblages in detail. Any additional dinocyst assemblage data I collected from other slides was purely to observe trends associated with ratios I recorded.

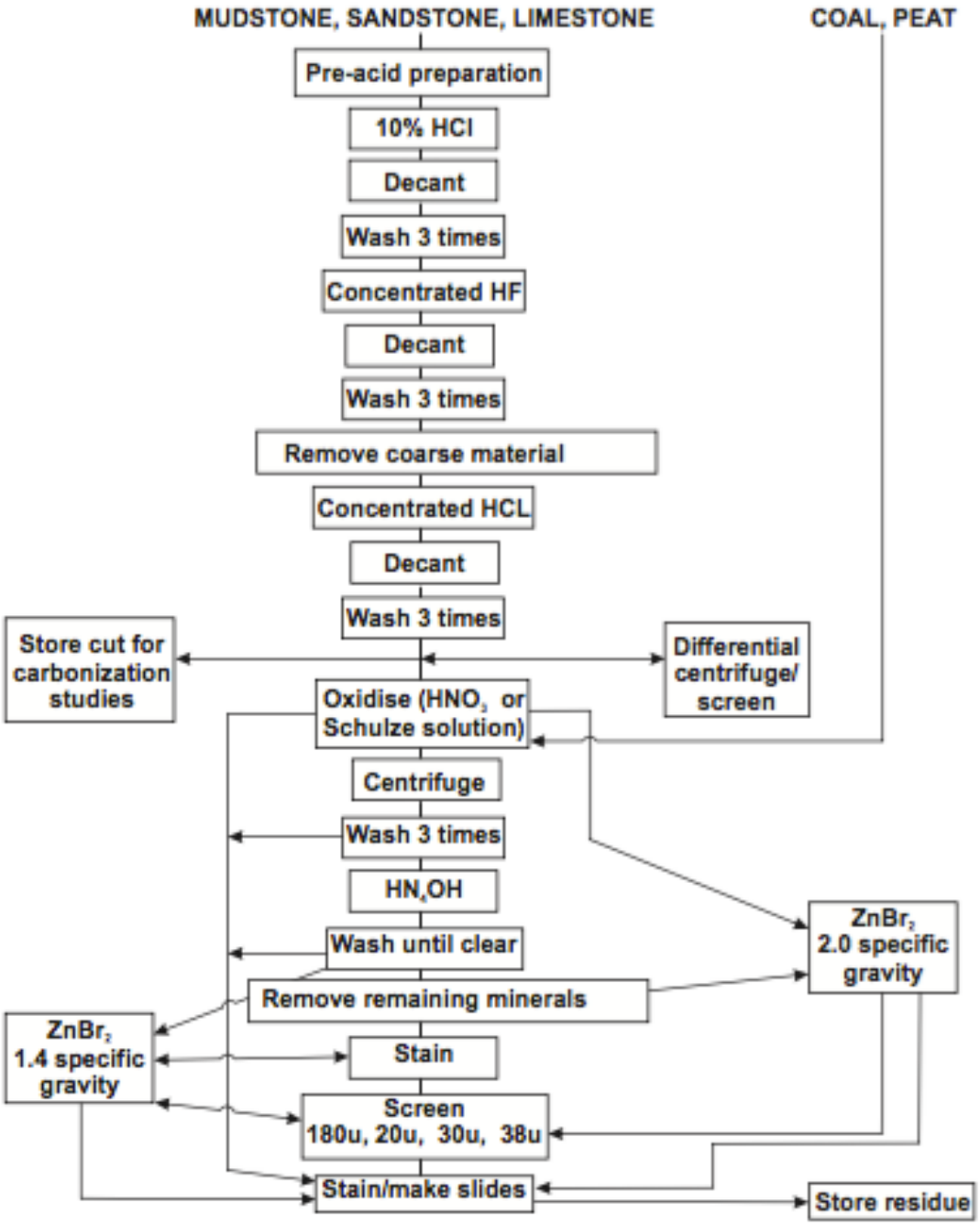

Figure 4.1 Flow chart showing the general processing technique used for preparing slides for palynogical analysis. [from Nohr-Hansen et al. 2016]

[5.0 Plates]

The following plates (1-6) include examples of most of the dinocyst taxa encountered in my section. All dinocysts are arranged in alphabetical order with red lines representing a scale of 10 µm unless otherwise noted. The designation "*sp"* represents a specimen that was not identified to species level. Most specimens were taken in the 40X view.

Plate 1

Figure 1. *Adnatosphaeridium vitattum*

Figure 2. *Adnatosphaeridium vitattum*

Figure 3. *Adnatosphaeridium vitattum*

Figure 4. *Adnatosphaeridium vitattum*

Figure 5. *Adnatosphaeridium* sp. Apical view

Figure 6. *Adnatosphaeridium* sp. Antapical view [same as fig. 5]

Figure 7. *Adnatosphaeridium vittatum*

Figure 8. *Adnatosphaeridium vittatum*

Figure 9. *Adnatosphaeridium vittatum*

Figure 10. *Adnatosphaeridium vittatum*

Figure 11. *Adnatosphaeridium vittatum*

Figure 12. *Cleistosphaeridium elegatulum*

Figure 13. *Areoligera gippingensis*

Figure 14. *Axiodinium* sp.

Figure 15. *Axiodinium* sp.

Figure 16. *Cerodinium glabrum*

Figure 17. *Cleistosphaeridium palmatum* [scale: 50um]

Figure 18. *Dapsilidinium* sp.?

Figure 19. *Cleistosphaeridium* sp.

Figure 20. *Cleistosphaeridium diversispinosum*

Plate 2

Figure 1. *Cleistosphaeridium elegatulum*

Figure 2. *Cleistosphaeridium elegatulum*

Figure 3. *Cleistosphaeridium elegatulum*

Figure 4. *Cleistosphaeridium elegatulum*

Figure 5. *Cleistosphaeridium ancryeum*

Figure 6. *Cleistosphaeridium ancryeum*

Figure 7. *Cleistosphaeridium diversispinosum*

Figure 8. *Cleistosphaeridium diversispinosum*

Figure 9. *Cleistosphaeridium diversispinosum*

Figure 10. *Cleistosphaeridium diversispinosum*

Figure 11. *Cordosphaeridium* sp.

Figure 12. *Cordosphaeridium gracile*

Figure 13. *Cordosphaeridium gracile*

Figure 14. *Cordosphaeridium delimurum*

Figure 15. *Cordosphaeridium delimurum*

Figure 16. *Cordosphaeridium delimurum* [scale: 50um]

Figure 17. *Cordosphaeridium delimurum*

Figure 18. *Cordosphaeridium cantharellus*

Figure 19. *Cordosphaeridium cantharellus*

Figure 20. *Cordosphaeridium cantharellus*

Plate 3

Figure 1. *Danea* sp.

Figure 2. *Danea* sp.

Figure 3. *Cordosphaeridium delimurum*

Figure 4. *Cordosphaeridium delimurum*

Figure 5. *Cordosphaeridium delimurum*

Figure 6. *Cordosphaeridium delimurum*

Figure 7. *Cordosphaeridium delimurum*

Figure 8. *Cordosphaeridium delimurum*

Figure 9. *Cordosphaeridium delimurum*

Figure 10. *Cordosphaeridium delimurum*

Figure 11. *Dapsilidinium pseudocalligerum*

Figure 12. *Dapsilidinium pseudocalligerum*

Figure 13. *Dapsilidinium pseudocalligerum*

Figure 14. *Deflandrea eocenica*

Figure 15. *Deflandrea eocenica*

Figure 16. *Deflandrea eocenica*

Figure 17. *Deflandrea eocenica*

Figure 18. *Deflandrea phosphoritica*

Figure 19. *Deflandrea* sp.

Figure 20. *Deflandrea* sp.

Plate 4

Figure 1. *Glaphyrocysta divaricata,* ventral surface

Figure 2. *Glaphyrocysta divaricata,* ventral view

Figure 3. *Glaphyrocysta divaricata*

Figure 4. *Glaphyrocysta divaricata*

Figure 5. *Glaphyrocysta divaricata*

Figure 6. *Spiniferites?* sp.

Figure 7. *Glaphyrocysta* sp.

Figure 8. *Glaphyrocysta* sp.

Figure 9. *Glaphyrocysta* sp.

Figure 10. *Glaphyrocysta* sp.

Figure 11. *Hafniaspheaera delicata*

Figure 12. *Spiniferites?* sp.

Figure 13. *Hystrichostrogylon* sp.

Figure 14. *Impagidinium* sp.*,* dorsal view (black arrow: apex)

Figure 15. *Impagidinium* sp.*,* ventral view [same as fig. 14]

Figure 16. *Impagidinium* sp.*,* ventral view

Figure 17. *Impagidinium* sp., dorsal view [same as fig. 16]

Figure 18. *Impagidinium* sp*.* (black arrow: apex)

Figure 19. *Impagidinium* sp*.* (black arrow: apex)

Figure 20. *Impagidinium* sp*.* (black arrow: apex)

Plate 5

Figure 1. *Lingulodinium funginum*

Figure 2. *Lingulodinium funginum*

Figure 3. *Dinocyst* indet.

Figure 4. *Lingulodinium funginum*

Figure 5. *Lingulodinium funginum*

Figure 6. *Lingulodinium funginum*

Figure 7. *Lingulodinium funginum*

Figure 8. *Lingulodinium funginum*

Figure 9. *Lingulodinium funginum*

Figure 10. *Lingulodinium funginum*

Figure 11. *Operculodinium?* sp.

Figure 12. *Lingulodinium funginum*

Figure 13. *Dapsilidinium pseuocolligerum*

Figure 14. *Dapsilidinium pseuocolligerum*

Figure 15. *Hafniasphaera* sp*.*

Figure 16. *Operculodinium centrocarpum,* archeopyle view [scale: 50um]

Figure 17. *Operculodinium centrocarpum,* ventral surface

Figure 18. *Operculodinium centrocarpum*

Figure 19. *Operculodinium centrocarpum*

Figure 20. *Operculodinium centrocarpum*

Plate 6

Figure 1. *Cleistosphaeridium diversispinosum,* apical operculum

Figure 2. *Palaeocystodinium bulliforme*

Figure 3. *Palaeoperidinium pyrophorum*

Figure 4. *Palaeoperidinium pyrophorum*

Figure 5. *Palaeoperidinium pyrophorum*

Figure 6. *Palaeoperidinium pyrophorum*

Figure 7. *Lentinia* sp.

Figure 8. *Lentinia* sp.

Figure. 9. *Rhombodinium* sp.

Figure 10. *Rottnestia borussica*

Figure 11. *Wetzeliella caviarticulata,* ventral surface

Figure 12. *Wetzeliella caviarticulata,* ventral view [same as fig. 11]

Figure 13. *Wetzeliella caviarticulata*

Figure 14. *Wetzeliella gochtii*

Figure 15. *Wetzeliella gochtii*

Figure 16. *Spiniferites* sp.

Figure 17. *Spiniferites* sp.

Figure 18. *Spiniferites* sp.

Figure 19. *Spiniferites* sp.

Figure 20. *Spiniferites* sp.

Plate 1

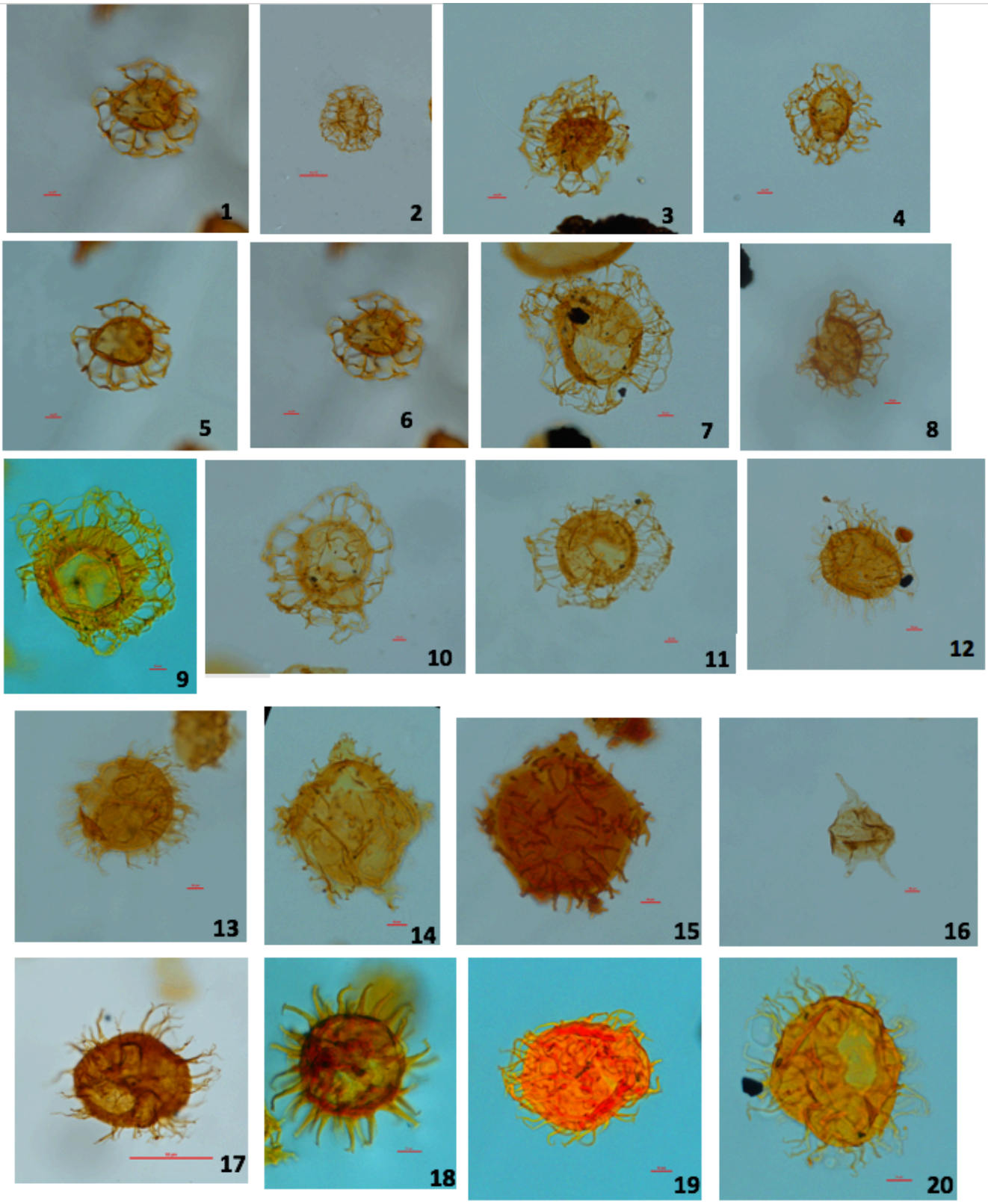

Plate 2

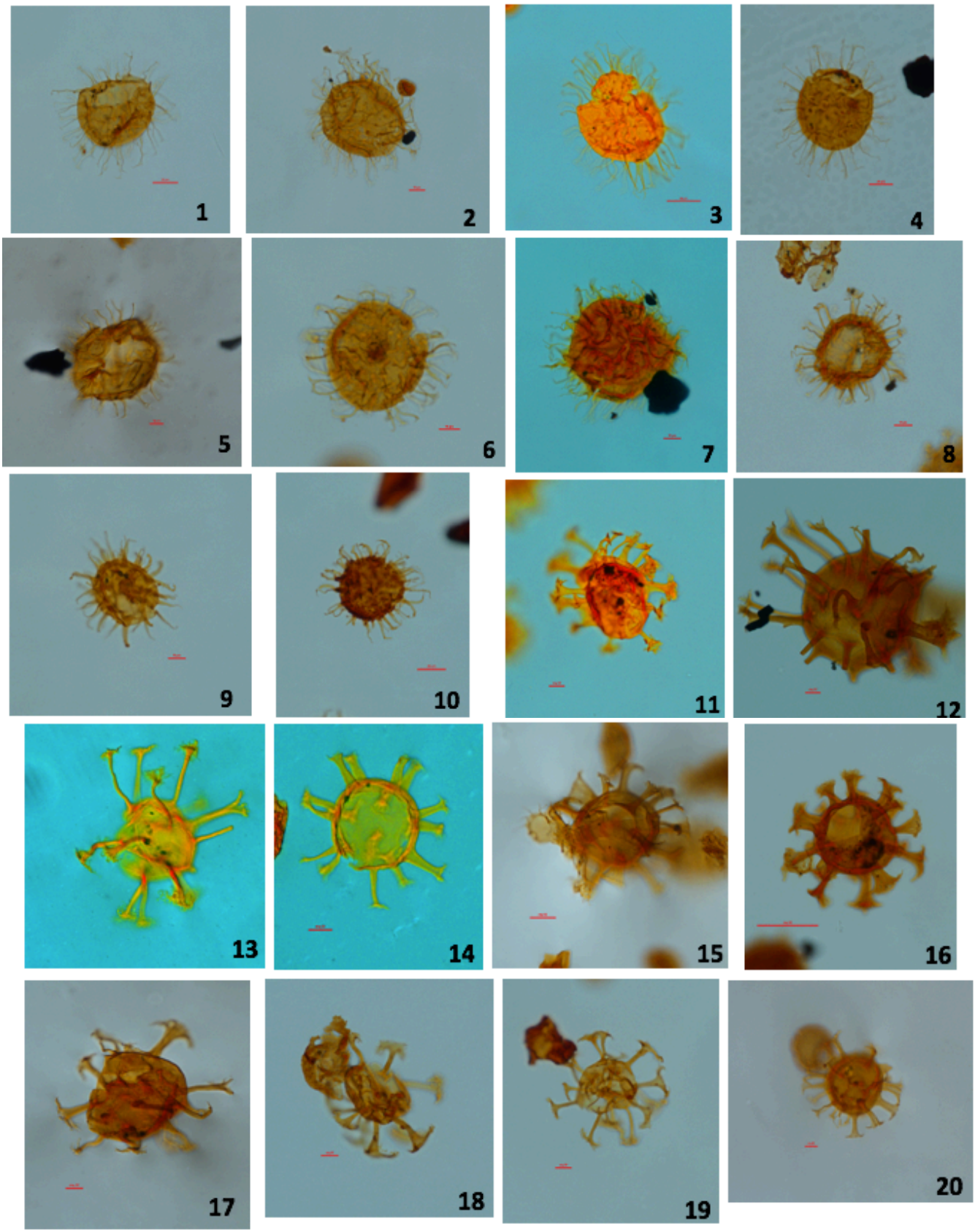

Plate 3

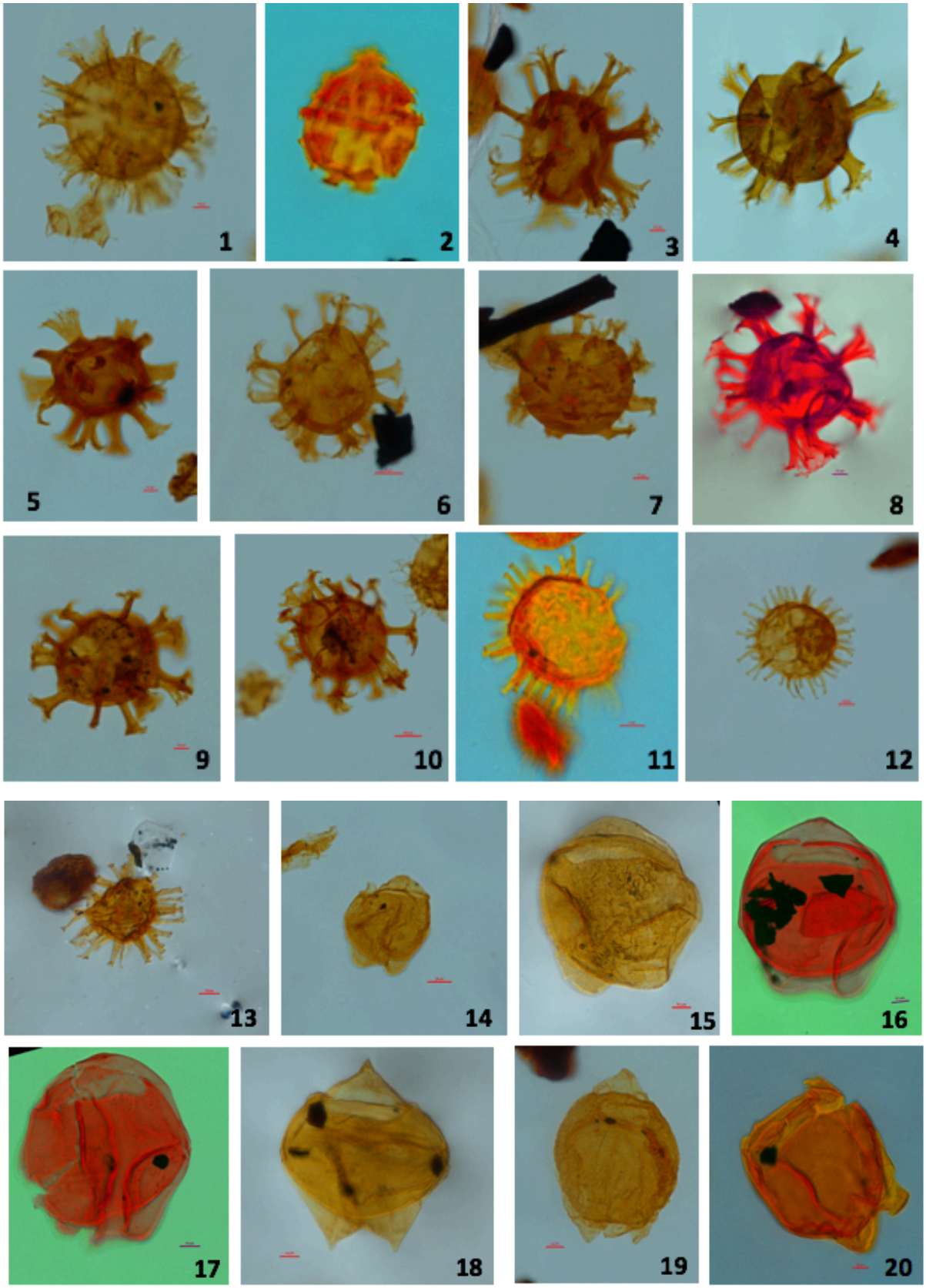

Plate 4

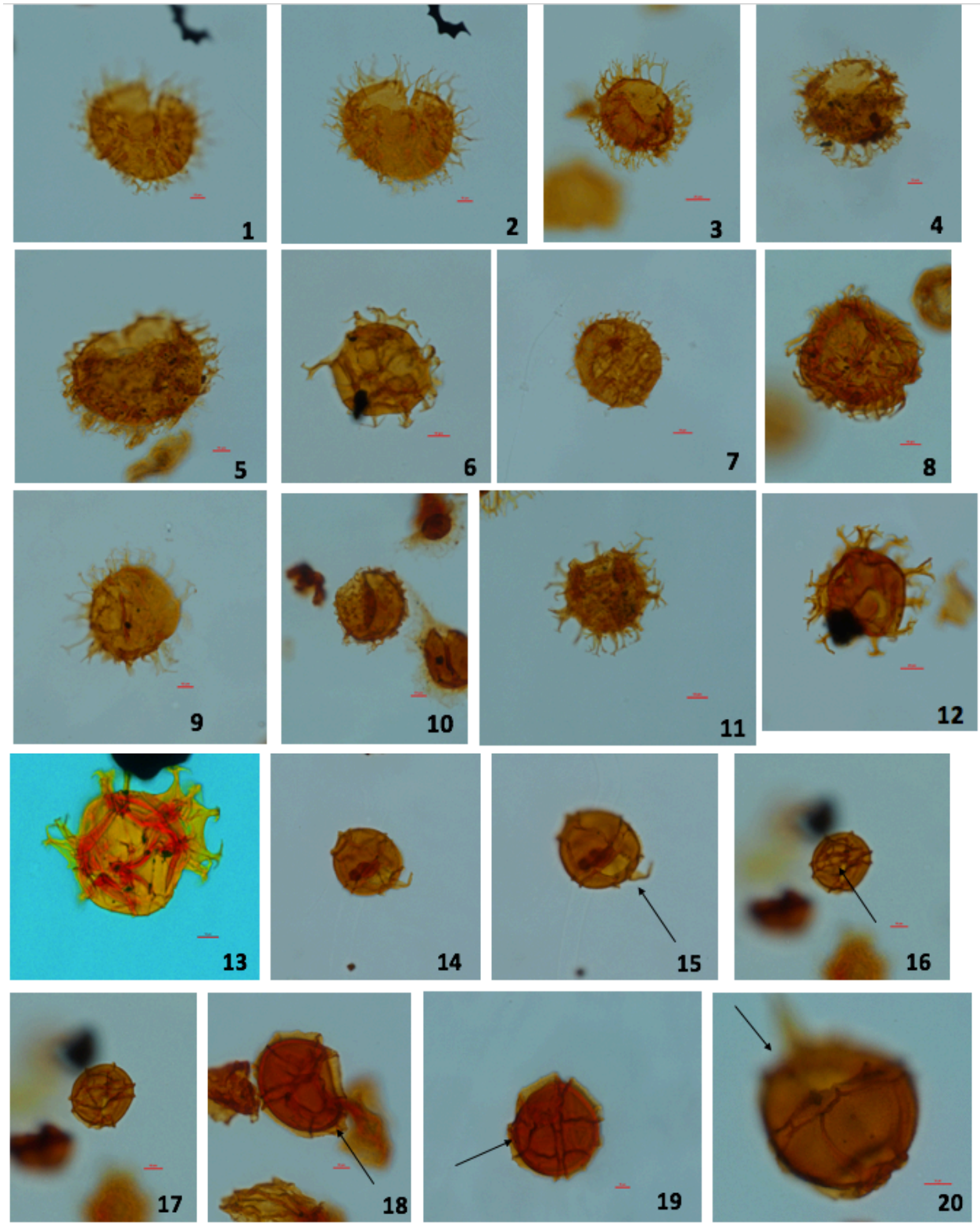

Plate 5

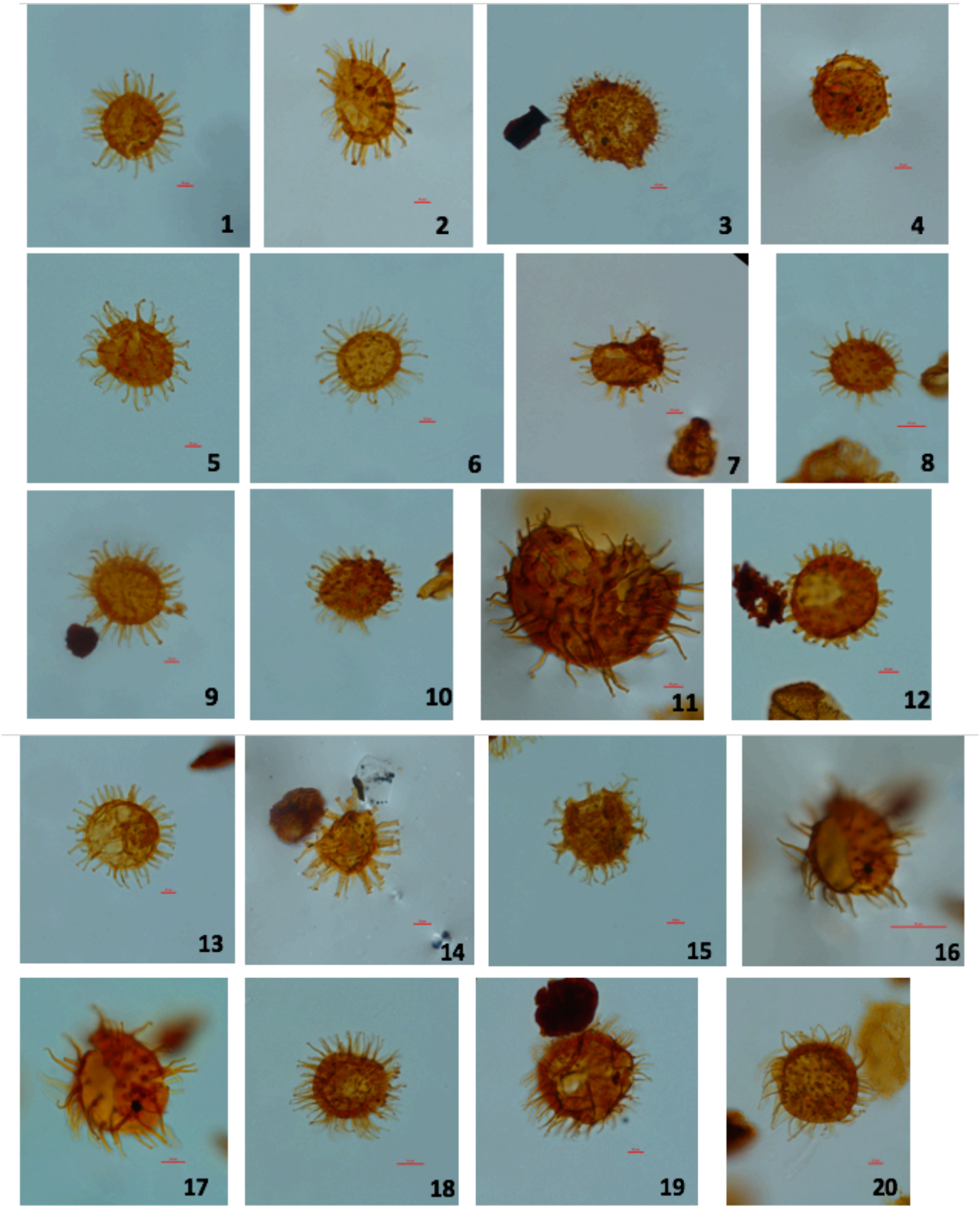

Plate 6

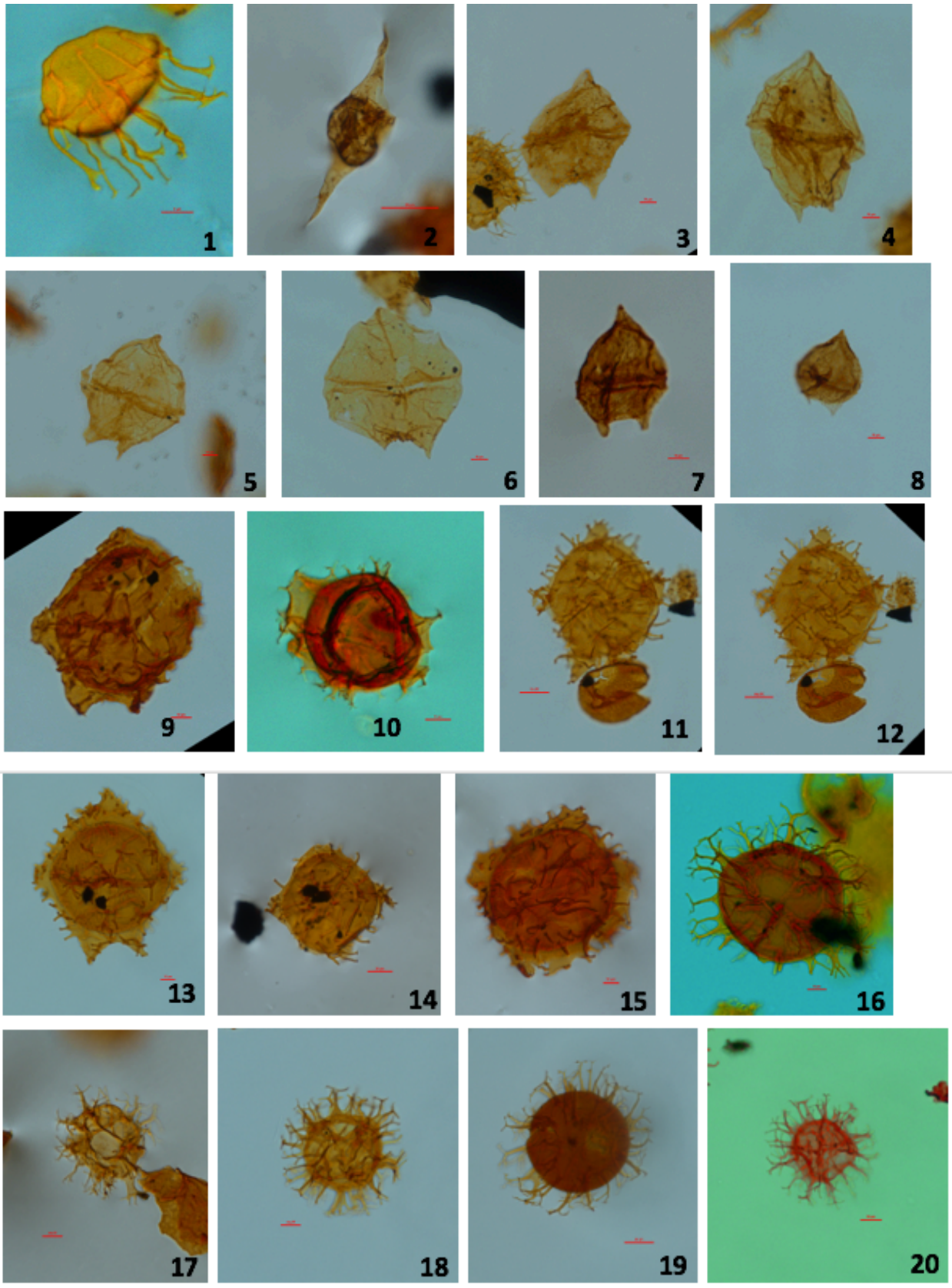

[6.0 Results & Datum Plots]

Table 6.1 Last occurrence plots. Slides arranged from oldest (bottom) to youngest (top).

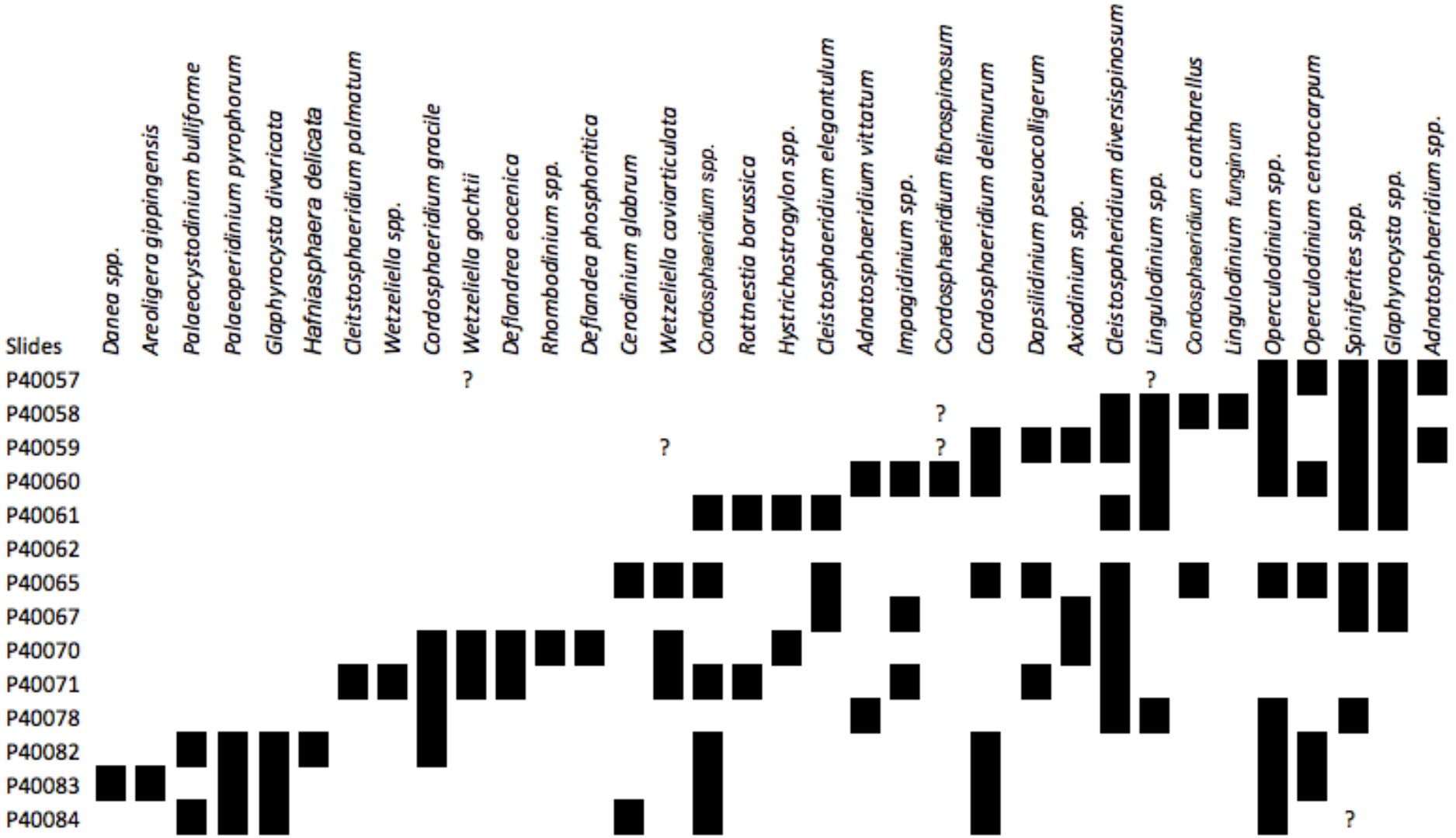

Table 6.2 First occurrence plots for well site 1276. Slides are arranged from oldest (bottom) to youngest (top)

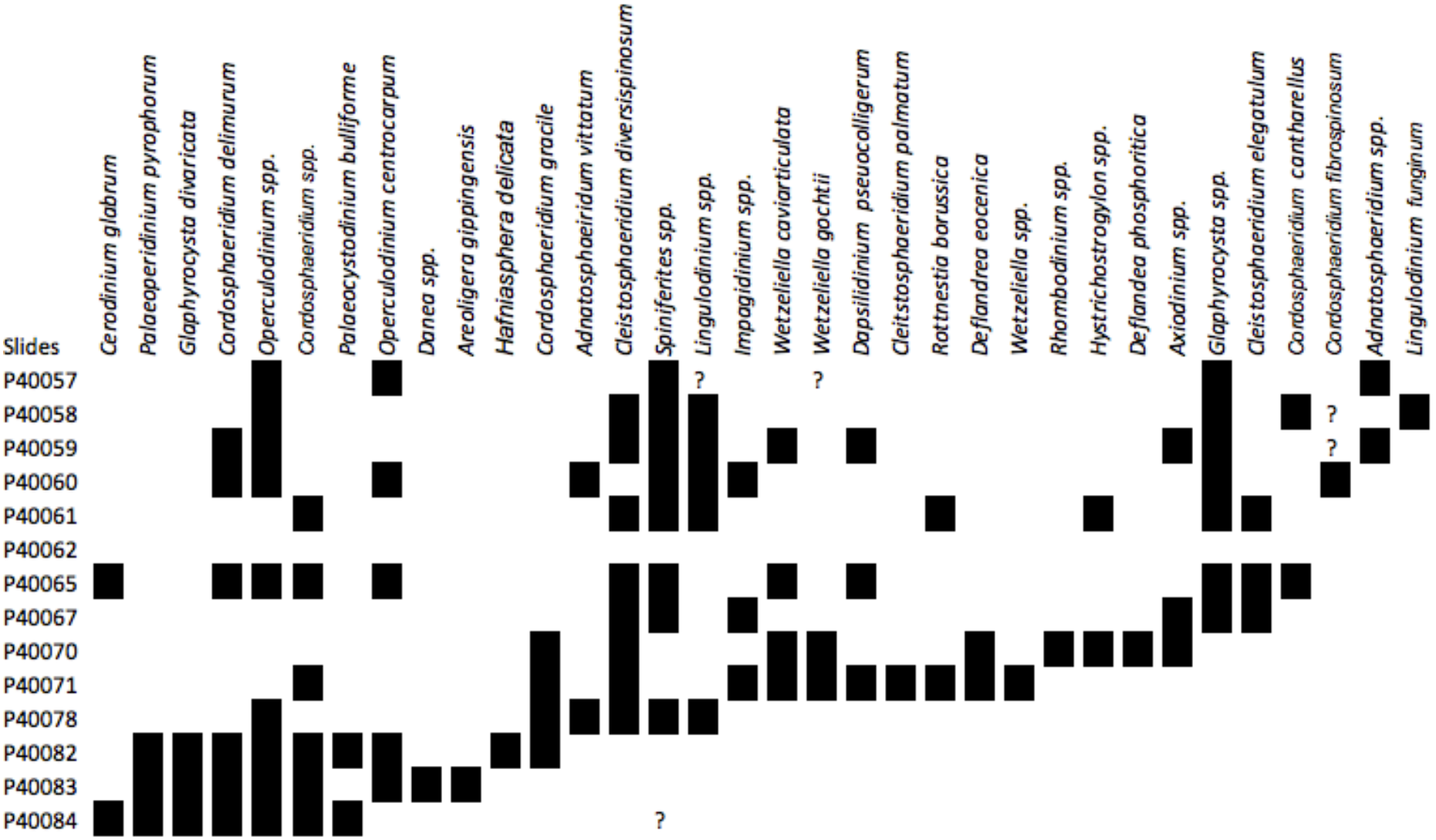

Tables 6.1 & 6.2 represent data plots that show both last occurrence (LO) and first occurrence (FO) receptively for site 1276. The data is organized by slide starting with the youngest at the top to oldest on the bottom. Slides P40084 to P40078 correlate to the series 16R-14R, and slides P40071 to P40057 correlate to series 8R-6R. It is important to note that some slides are missing between the two series. However, this does not hinder the ability to draw conclusions based on the observed trends. Question marks represent a section where a certain species tentatively occurs. Preservation was generally moderate to good throughout the section, although some dinocysts were deformed, making identification difficult.

Dinocysts throughout the Paleogene section are relatively diverse. Abundance of dinocysts from the bottom to top of the section show strong correlation with those shown by Sluijs et al. (2004), where dinocyst species diversity shows a localized peak at the Paleocene/Eocene boundary. Abundances of particular genera and species also show generalized trends. The lower section (slides P40084 to P40078) features a high degree of diversity as well as a spike in general abundance. It is characterized by abundant specimens of *Glaphyrocysta,* as well as age-diagnostic genera such as *Cerodinium, Palaeoperidinium* and *Palaeocystodinium bulliforme*. *Glaphyrocysta* abundances are greater in the lower part of the section, and the reverse is true with *Spiniferites,* which tends to increase in abundance up-section. The middle of the section (slides P40071 to P40062) is represented by an increase in *Wetzeliella* as well as *Rhombodinium* and *Axiodinium,* all in the subfamily Wetzelielloideae [Williams et al. 2016]. *Impagidinium* also shows a localized spike through slides P40071 to P40067. The upper section at Site 1276 (slides P40061-P40057) is defined by high abundances in *Spiniferites, Lingulodinum,* and *Cordosphaerdium*, although *Cordosphaerdium* varies greatly throughout the section.

P-Cyst/G-Cyst ratios show a major spike near the middle of the section (slides P40071 & P40070). The ratio tends to be low through the rest of the section. Crouch et al. (2001) reports on a global event associated with the genus *Apectodinium,* where assemblages can be linked to the PETM and reflect a worldwide synchronous event representing a global increase in sea surface productivity. *Apectodinium* was not found at Site 1276 during the present study.

Table 6.3 P-Cyst versus G-cyst percentage for each observed slide through the well site 1276 Paleogene section. Red represents the localized spike in P Cyst assemblages and their relative percentages in two samples (P40070 and P40071).

Column1	P Cyst %	G Cyst %
P40057-02	14	86
P40058-02	11	89
P40059-02	15	85
P40060-02	4	96
P40061-02	0	100
P40062-02	barren	barren
P40065-02	7.5	92.5
P40067-02	7.5	92.5
P40070-02	53	47
P40071-02	43	57
P40078-02	0	100
P40082-02	12	88
P40083-03	23	77
P40084-02	17	83

[7.0 Discussion]

Key biostratigraphic taxa have been identified throughout the Paleogene section at Site 1276. Using these taxa, ages can be determined for individual samples and paleoenvironmental interpretations can be made. Last occurrences (LOs) and first occurrences (FOs) of individual taxa provide most of the evidence for age determination, although because most previous work in the region is based on cuttings samples, the LOs are better known in offshore eastern Canada. Some dinocyst genera are less useful than others for age determination because they are long ranging. Events used here are based on those provided by Fensome et al. (2008), Fensome et al. (2016), and Nohr-Hansen et al. (2016).

Slides P40084 to P40082 contain key dinocyst taxa that occur in single samples or throughout the interval. *Danea spp.* (LO of late Selandian) is seen in small numbers in sample P40083. *Palaeocystodinium bulliforme* and *Palaeoperidinium pyrophorum* are both excellent indicators of the late Selandian and both show high abundance levels and LO's in slide P40082. Using these key species, the youngest age for P40082 is late Selandian to possibly early Thanetian as seen through *Glaphyrocysta divaricata* although reported by Fensome et al. (2009) to have a LAD of Lutetian on the Scotian Margin its common LAD is Thanetian. The early Selandian is constrained by the presence of *Cerodinium glabrum* which only occurs in sample P40084 and lower. *Ceredonium glabrum* typically extends well into the Thanetian so this species does not constrict any age within the section, however provides a good marker for the late Paleocene. It also occurs higher in the section, in sample P40065, but other taxa in the assemblage suggest that *Cerodinium glabrum* is reworked in that sample. Although interpreted by the Shipboard Scientific Party to be near the Paleocene/Eocene boundary, Sample P40078 contains no observed age-diagnostic dinocysts.

As noted, slides of samples from the early Eocene were reported barren by Tucholke et al. (2004) and were not available in the present study. Higher samples through the lower to upper Eocene were provided, however. The FO of the wetzelielloids *Wetzeliella*, *Rhombodinium and Axiodinium* in sample P40071 suggest that this part of the section lies within the middle Eocene. Samples P40071 and P40070 have a spike in *Delandrea eocenica*, which has an LO of middle Lutetian. The presence of *Wetzeliella caviarticulata* (LO of early Lutetian) occurs higher

up, in sample P40065. This can be interpreted as evidence of reworking as *Deflandrea eocenica* has a LO much lower in the section. Slide P40065 also contains a specimen of *Cerodinium diebelii,* providing more evidence for reworking. The presence of *Cordosphaeridium gracile* (LO of early Lutetian) and *Cleistosphaeridium palmatum* (LO of late Ypresian) indicate that sample P40071 is late Ypresian to early Lutetian. The high abundance and local peak in *Deflandrea eocenica* in sample P40070 indicates a minimum middle Lutetian.

Slides P40067 to P40060 contain a relatively uniform dinocyst assemblages, although certain LOs indicate ages and evidence of reworking. An exception is sample P40062, which had no well preserved, recognizable dinocysts and thus is reported to be inadequate in providing reasonable conclusions. The absence of well-preserved specimens in that sample may be because the sample is in a carbonate bed (most likely a debris flow deposit). The presence of *Adnatosphaeridium vittatum* (LO of late Bartonian) in sample P40060, as well as the presence of *Hystrichostrogylon spp.,* occurring in sample in P40061 (LO of Bartonian-Priabonian) are two good index taxa. Although *Cordosphaeridium delimurum* (LO of early Lutetian) occurs higher up, in sample P40059, its abundance is extremely low compared to that in earlier samples, and it occurs sporadically, suggesting reworking. *Dapsilidinium pseudocolligerum* (LO of Tortonian) is also associated with and last appears in sample P40059. While this species has an LAD of Miocene (Tortonian), it is common in the late Eocene and thus agrees with my findings [R.A Fensome, personal communication]. Using these key species an age top of Bartonian can be applied to sample P40059.

Samples P40058 and P40057 at the top of the section contain no useful dinocysts. It is thus assumed that the top of the Paleogene is not seen in the interval studied. The taxa observed within these top two sections are long ranging and extend into the Oligocene or the Miocene in some cases. The only species worth noting is *Lingulodinium funginum,* which only occurs in slide P40058 in high abundance. The reason for the occurrence of this species is most likely related to paleoenvironment.

[7.1 Paleoenvironments: a Discussion]

The dinocyst assemblages in samples from the Paleogene section at Site 1276 show general paleoenvironmental trends. At the Paleocene/Eocene boundary, *Apectodinium* is absent. This can be hypothesized to be because of the higher latitude of the site, with *Apectodinium* being more prominent at lower latitudes [Bujak & Brinkhuis, 1998]. However, *Apectodinium* is reported to show spikes along the Grand Banks, and thus the absence from my section may be attributed to missing samples, from the late Thanetian to late Ypresian [R.A Fensome personal communication].

High abundances of *Cordosphaeridium* coupled with the greater abundance of *Glaphyrocysta* in the lower part of the section (slides P40084 to P40078) is indicative of an outer neretic setting with some inner neritic influence. Perhaps warmer climates leading up the Paleocene/Eocene transition resulted in more coastal influence. The opposite is seen the abundance of *Spiniferites*, which shows an increase of abundance near the section's top (late Eocene), indicating a drop in temperature after the Paleocene/Eocene thermal maximum as well as the middle Eocene climatic optimum. Sluijs et. al (2008) argued that a high S/A ratio (*Spiniferites*/ *Spiniferites* + *Areoligera*) indicated outer neritic environments and a low ratio indicated inner neritic. Here, *Glaphyrocysta* is counted with *Areoligera* as it is closely related. There is a clear increase in S/A ratio up section, which agrees with the proposed hypothesis of an outer neretic paleoenvironment with inner neritic influence brought on by climatic highs through the early to middle Eocene.

The P-Cyst: G-cyst ratio, as proposed by Harland (1973), and is based on the notion that if G-cysts are more abundant than P-cysts in more open-marine settings [Nohr-Hansen et al. 2016]. The large localized spike in P-Cyst assemblages as seen in table 6.3 near what is proposed to be Lutetian in age is represented by a large influx of inner-neretic genera such as *Deflandrea, Wetzeliella* and *Cleistosphaeridium* into an outer neritic system (figure 7.1). As outlined in Sluijs et al. (2005) the warming associated with the Paleocene/Eocene thermal maximum could have probably created higher nutrient influxes into outer neritic settings as a result of higher terrigenous productivity. The missing early Eocene section creates some uncertainty in this interpretation.

The presence of *Impagidinium,* which occurs only within the middle Eocene section at Site 1276, indicates an outer-neritic setting bordering an oceanic setting. *Impagidinium* could have been brought into the system through upwelling processes and/or wind [Pross & Brinkhuis 2005].

PALEOENVIRONMENTAL PREFERENCES OF DINOCYST TAXA IN THE LABRADOR- BAFFIN SEAWAY

Coastal/Marginal Marine	Inner Neritic	Outer Neritic	Open Ocean
Nyktericysta *Homotryblium* *Eocladopyxis* *Polysphaeridium* *Tuberculodinium* *Micrhystridium* (A) *Heteraulacacysta* *Vesperopsis*	*Deflandrea* *Wetzeliella* *Glaphyrocysta* *Areoligera* *Micrhystridium* (A) *Cleistosphaeridium* *Dinogymnium* *Heterosphaeridium* *Phthanoperidinium* *Cribroperidinium*	*Spiniferites* *Hystrichosphaeridium* *Cordosphaeridium* *Hystrichokolpoma* *Cleistosphaeridium* *Operculodinium* *Phelodinium* *Cerodinium*	*Impagidinium* *Nematosphaeropsis* *Pterodinium* *Cannosphaeropsis*

Figure 7.1 Palaeoenvironmental preference chart for coastal, inner neretic, outer neretic and oceanic dinoflagellates. [from Nohr-Hansen et al. 2016].

[8.0 Conclusions]

Analysis of the dinocyst assemblages from 14 samples at Site 1276 has led to age determinations and paleoenvironmental interpretation. Dinocyst assemblages can be divided into three intervals, early Selandian to Thanetian, late Ypresian to middle Lutetian, and middle Lutetian to early Priabonian. Evidence for reworking has also been found throughout the section and was most likely induced by debris flows, resulting in turn from climatic highs. Dinocyst abundances agree with previous studies in suggesting greater taxonomic diversity near the Paleocene/Eocene boundary before decreasing in the Eocene.

Dinocysts are more abundant through the late Paleocene section and decrease up-section into the Eocene. *Glaphyrocysta* shows significantly higher numbers compared to *Spiniferites* near the base of the section, with the opposite occurring near the top. P-cysts show a spike near the middle of the section, in an interval interpreted to be early to middle Lutetian in age. This spike has been linked to climate dynamics, perhaps related to the Paleocene-Eocene Thermal Maximum, and possibly the mid Eocene climatic optimum. Ultimately, it is apparent that higher global temperatures are seen through dinocyst assemblages throughout the Paleogene section of site 1276.

Key age diagnostic dinocysts have been found within the section. *Palaeocystodinium bulliforme* and *Palaeoperidinium pyrophorum* provide good age constraints for the top of the middle Paleocene. The peak in *Deflandrea eocenica* and appearance of particular wetzelielloids in the middle part of the section provide good age constraints for the middle Lutetian. The presence of *Adnatosphaeridium vittatum* in high abundances near the sections top is used as an index taxon for the Bartonian. Reworking is seen though the presence of *Cerodinium glabrum* which occurs significantly higher up in the section within the Eocene which contradicts what age contraints suggest. Ages cannot be determined for the top two samples because all assemblages are composed of species that range up into the Oligocene and Miocene.

The paleoenvironmental setting has been interpreted as outer-neritic bordering an oceanic setting throughout most of the Paleogene. The presence of *Impagidinium* throughout the middle Eocene within the section indicates influence of oceanic environments. Inner-neritic influence during the Thanetian and Lutetian is shown through the reworking of various

dinocysts, indicating higher terrigenous productivity. The local spike in P-cyst assemblages near the middle Lutetian indicates with some uncertainty that input of inner neritic species could have been influenced by high climates seen through the Paleocene-Eocene, which saw a drastic rise in oceanic temperatures. This rise in ocean temperatures would have influenced P-Cyst productivity throughout the early Eocene following the PETM. This spike may also be attributed to the mid Eocene climatic optimum though an entire early Eocene section was missing from observed samples.

References

Barrs, M.S., & Williams, G.L. (1973). Palynology and nannofossil processing techniques. Geological Survey of Canada, Paper 73-26, 25 p.

Bujak, J.P., and Brinkhuis, H. 1998. Global warming and dinocyst changes across the Paleocene/Eocene epoch boundary. In: Aubry, M.-P. *et al.* (eds): Late Paleocene- early Eocene climatic and biotic events in the marine and terrestrial records, 277-295.

Crouch, E.M., Hellmann-Clausen, C., Morgans, Hugh E.G., Rogers, Karyne, M. Rogers., Egger, H., Shmitz, B. 2001. Global dinoflagellate event associated with the late Paleocene thermal maximum. *Geology,* vol. 29: no. 4: p. 315-318.

Evitt, W.R. 1961. Observations on the Morphology of Fossil Dinoflagellates. Micropaleontology, 29(4): pp. 385-420.

Fensome R.A., Nohr-Hansen, H., Williams, G.L. 2016. Cretaceous and Cenozoic Dinoflagellate cysts and other palynomorphs from the western and eastern margins of the Labrador-Baffin Seaway. *Geological Survey of Denmark and Greenland Buleten 36,* 143 p.

Fensome R.A, Saldarriaga J.F. & Taylor F.J.R. (1999) Dinoflagellate phylogeny revisited: reconciling morphological and molecular based phylogenies, Grana, 38:2-3, 66-80, doi: 10.1080/00173139908559216

Fensome, R.A., MacRae, R.A. and Williams, G.L. 2008. DINOFLAG2, Versian 1. American Association of Stratigraphic Palynologists, Data Series No.1.

Fensome, R.A., Williams, G.L., Macrae, R.A. 2009. Late Cretaceous and Cenozoic fossil dinoflagellates and other Palynomorphs from the Scotian Margin, Offshore Eastern Canada. *Journal of Systematic Palaeontology* 7(1): 1-79.

Fensome, R.A., Riding, J.B. & Taylor, F.J.R. 1996. Chapter 6. Dinoflagellates; in: Jansonius, J. & McGregor, D.C. (ed.), Palynology: principles and applications; American Association of Stratigraphic Palynologists Foundation, Vol. 1, p. 107-169.

Fensome, R., MacRae, R., Moldowan, J., Taylor, F., & Williams, G. 1996. The Early Mesozoic Radiation of Dinoflagellates. *Paleobiology*, 22(3), pp. 329-338.

Fensome, R., Crux, J., Gard, G., MacRae, A., Williams, G., Thomas, F., Fiorini, F., & Wach, G. (2008). The last 100 million years on the Scotian Margin, offshore eastern Canada: an event-stratigraphic scheme emphasizing biostratigraphic data. *Atlantic Geology, 44*(1), Pages 93 - 126. doi: http://dx.doi.org/10.4138/6506

Nøhr-Hansen, H., Williams, G.L., & Fensome, R.A. (In Press), Biostratrigraphic correlation of the western and eastern margins of the Labrador-Baffin Seaway and Implications ofr the regional geology. Geological Survey of Denmark and Greenland, v. 37, 74 p.

Pross, J. & Brinkhuis, H. 2005. Organic-walled dinoflagellate cysts as paleoenvrionmental indicators in the Paleocene; a synopsis of concepts. Palaontol Z. 79(1): 53-59.

Sluijs, A & Brinkhuis, H. 2009. A dynamic climate and ecosystem state during the Paleocene-Eocene Thermal Maximum: inferences from dinoflagellate cyst assemblages on the New Jersey Shelf. *Biogeosciences,* 6, p. 755-1781.

Sluijs, A., Pross, J., & Brinkhuis, H. 2005. From greenhouse to icehouse; organic-walled dinoflagellate cysts as paleoenvironmental indicators in the Paleogene. *Earth Science Reviews*, 68, p. 281-315, doi:10.1016/j.earscirev.2004.06.001.

Sluijs, A., et al. 2008. Eustatic variations during the Paleocene-Eocene greenhouse world. *Paleooceanography*, 23, PA4216, doi:10.1029/2008PA001615.

Shipboard Scientific Party, 2004. Leg 210 summary. *In* Tucholke, B.E., Sibuet, J.-C., Klaus, A., et al., *Proc. ODP, Init. Repts.,* 210: College Station, TX (Ocean Drilling Program), 1–78. doi:10.2973/odp.proc.ir.210.101.2004

Shipboard Scientific Party, 2004. Site 1276. *In* Tucholke, B.E., Sibuet, J.-C., Klaus, A., et al., *Proc. ODP, Init. Repts.,* 210: College Station, TX (Ocean Drilling Program), 1–358. doi:10.2973/odp.proc.ir.210.103.2004

Tucholke, B.E., Sawyer, D.S., & Sibuet J.-C. 2007. Breakup of the Newfoundland-Iberia rift. Geological Society London Special Publications. doi: 10.1144/SP282.2.

Tucholke, B.E., Sibuetm J.-C., & Klaus, A. Leg 210 Synthesis: Tectonic, Magmatic, and Sedimentary Evolution of the Newfoundland-Iberia Rift. *Proceedings of the Ocean Drilling Program, Scientific Results,* vol. 210.

Williams, G.L., Fensome, R.A., Brinkhuis, H., & Pross, J. (2009), The Paleobiology of Dinoflagellates. Unpublished revised for the dinoflagellate short course in Urbino Italy.

Williams G.L., Damassa, S.P., Fensome, R.A., & Guerstein, R. 2015. *Wetzeliella* and its allies – the 'whole' story: a taxanomic revision of the Paleogene dinoflagellate subfamily Wetzelielloideae. *Palynology*, 39(3), p. 289-344. http://dx.doi.org/10.1080/01916122.2014.993888.

Zachos J., Pangani, M., Sloan, L., & Thomas, E. 2001. Trends, Rhythms, and Aberrations in Global Climate 65 Ma to Present. *Science*, vol. 292, p. 686-693.

Zachos J., Dickens, G.R., & Zeebe R.E. 2008. An early Cenozoic perspective on greenhouse warming and carbon-cycle dynamics. *NATURE*, vol. 45, p.279-283. doi:10.1038/nature06588.

Appendix A: Sample Counts & Analysis

Slide Series Reference Table:

Slides	Corresponding Series
P40057-02	6R-3
P40058-02	6R-4
P40059-02	6R-5
P40060-02	6R-6
P40061-02	7R-1
P40062-02	7R-2
P40065-02	7R-5
P40067-02	8R-1
P40070-02	8R-4
P40071-02	8R-5
P40078-02	14R-1
P40082-02	16R-1
P40083-03	16R-2
P40084-02	16R-3

Core Description (My section) [From: Shipboard Scientific Party]

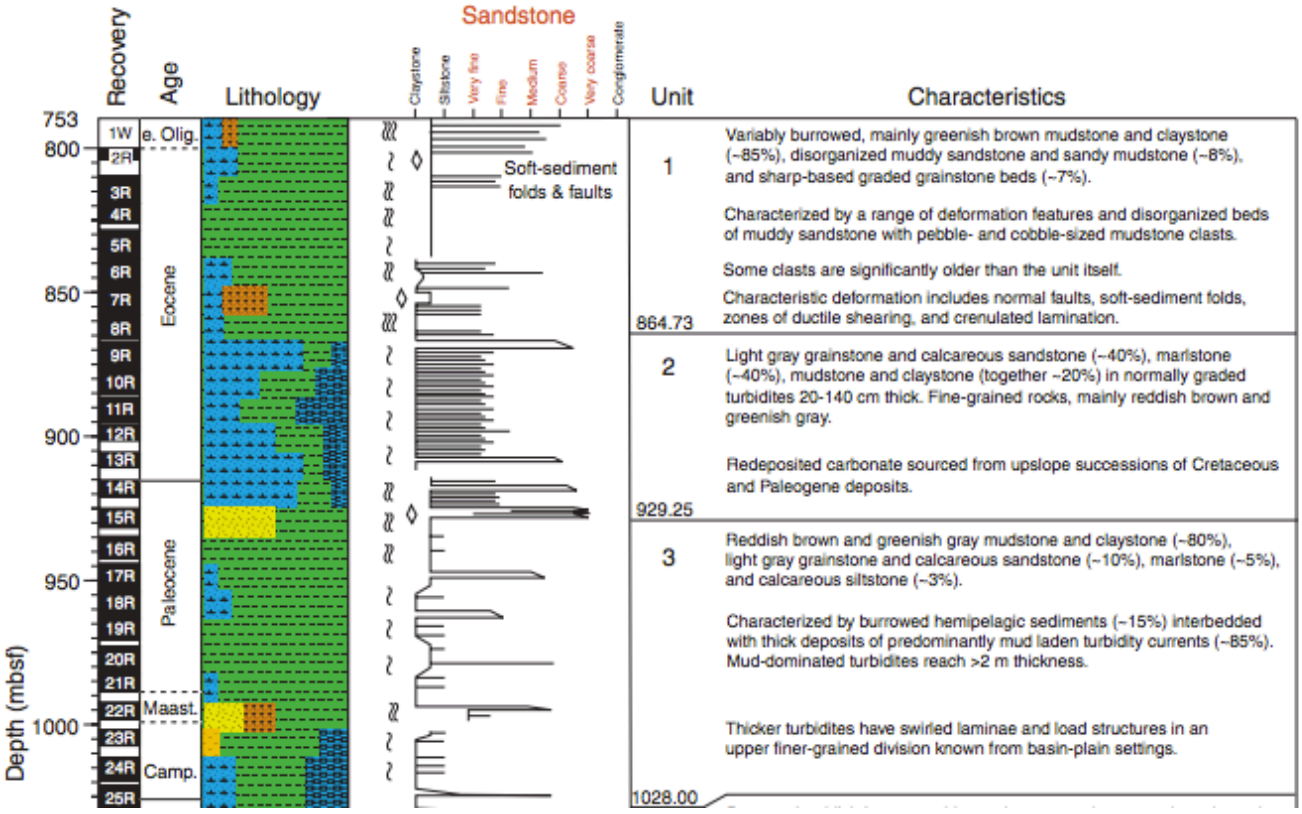

Sample Abundance Counts Table:

	Genus																			
Slide	*Achomasphera*	*Adnatosphaeridium*	*Areoligera*	*Axiodinium*	*Cerodinium*	*Cordosphaeridium*	*Danea spp.*	*Damassadinium*	*Deflandrea*	*Glaphyroysta*	*Hafniasphera*	*Hystrichostrogylon*	*Impagidinium*	*Linguludinium*	*Operculodinium*	*Palaeocystodinium*	*Rhombodinium*	*Palaeoperidinium*	*Rottnestia*	*Spiniferites*	*Wetzeliella*
P40057-02										3					3					7	1
P40058-02		1				3	2			1				11	1			2		5	
P40059-02		5		1		1	1			3				1						2	1
P40060-02		1				2				1			3	2	1					9	
P40061-02						1	3			1				2					1	3	
P40062-02																					
P40065-02					1	4	3			2					1					7	1
P40067-02				1			3			1			1							4	
P40070-02				1		1	1		8			1	3				1				2
P40071-02						2	1		1				7		1				1		7
P40078-02	1	4				5	1							1	3					4	
P40082-02						9				6	1				3	1		3			
P40083-03			1			12		2		5					3			5			
P40084-02					3	26	4			28						2		11		4	
Total	1	11	1	3	4	66	19	2	9	51	1	1	14	17	16	3	1	21	2	45	12

P-Cyst/G-Cyst Ratio Counts:

	Peridiniineae	Gonyaulacineae	**Ratio**
P40057-02	3	18	6
P40058-02	3	25	8.333333333
P40059-02	3	17	5.666666667
P40060-02	1	25	25
P40061-02	0	14	
P40062-02	barren	barren	
P40065-02	2	24	12
P40067-02	1	12	12
P40070-02	8	7	0.875
P40071-02	9	12	1.333333333
P40078-02	0	18	
P40082-02	3	22	7.333333333
P40083-03	5	17	3.4

Appendix B: Dinoflagellate Index – Authorships (From DINOFLAJ3)

ADNATOSPHAERIDIUM - Williams, G.L. and Downie, C., 1966c: Further dinoflagellate cysts from the London Clay. In: Davey, R.J., Downie, C., Sarjeant, W.A.S. and Williams, G.L., Studies on Mesozoic and Cainozoic dinoflagellate cysts; British Museum (Natural History) Geology, Bulletin, Supplement 3, p.215-236.

AREOLIGERA - Williams, G.L. and Downie, C., 1966c: Further dinoflagellate cysts from the London Clay. In: Davey, R.J., Downie, C., Sarjeant, W.A.S. and Williams, G.L., Studies on Mesozoic and Cainozoic dinoflagellate cysts; British Museum (Natural History) Geology, Bulletin, Supplement 3, p.215-236.

AXIODINIUM - Fensome, R.A., Williams, G.L. and MacRae, R.A., 2009: Late Cretaceous and Cenozoic fossil dinoflagellates and other palynomorphs from the Scotian Margin, offshore eastern Canada. Journal of Systematic Palaeontology, v.7, no.1, p.1-79, pl.1-11

CERODINIUM - Fensome, R.A., Williams, G.L. and MacRae, R.A., 2009: Late Cretaceous and Cenozoic fossil dinoflagellates and other palynomorphs from the Scotian Margin, offshore eastern Canada. Journal of Systematic Palaeontology, v.7, no.1, p.1-79, pl.1-11.

CLEISTOSPHAERIDIUM - Davey, R.J., Downie, C., Sarjeant, W.A.S. and Williams, G.L., 1966: VII. Fossil dinoflagellate cysts attributed to *Baltisphaeridium*.

CORDOSPAERIDIUM - Eisenack, A., 1963b: *Cordosphaeridium* n.g., ex *Hystrichosphaeridium*, Hystrichosphaeridea. Neues Jahrbuch für Geologie und Paläontologie, Abhandlungen, v.118, p.260-265, pl.29.

DANEA - Drugg, W.S., 1970b: Some new genera, species, and combinations of phytoplankton from the Lower Tertiary of the Gulf Coast, U.S.A. Proceedings of the North American Paleontological Convention, Chicago, September 1969, part G, p.809-843.

DAPSILIDINIUM - Bujak, J.P., Downie, C., Eaton, G.L. and Williams, G.L., 1980: Dinoflagellate cysts and acritarchs from the Eocene of southern England. Special Papers in Palaeontology, no.24, 100 p., pl.1-22.

DEFLANDREA - Eisenack, A., 1938b: The Phosphorite Nodules of Amber Formation as the Suppliers of Tertiary Plankton. Writings of the Physico-Economic Society of Königsberg, v.70, no.2, p.181-188.

GLAPHYROCYSTA - Stover, L.E. and Evitt, W.R., 1978: Analyses of pre-Pleistocene organic-walled dinoflagellates. Stanford University Publications, Geological Sciences, v.15, 300 p.

HAFNIASPHERA - Hansen, J.M., 1977: Dinoflagellate stratigraphy and echinoid distribution in Upper Maastrichtian and Danian deposits from Denmark. Bulletin of the Geological Society of Denmark, v.26, p.1-26.

HYSTRICHOSTROGYLON - Agelopoulos, J., 1964: Hystrichostrogylon membraniphorum n.g. N.sp. From the Heiligenhafen Kieselton (Eocene). New Year's Book for Geology and Paleontology, Monatshefte, no.11, p.673-675.

IMPAGIDINIUM - Stover, L.E. and Evitt, W.R., 1978: Analyses of pre-Pleistocene organic-walled dinoflagellates. Stanford University Publications, Geological Sciences, v.15, 300 p.

LINGULODINIUM - Wall, D., 1967: Fossil microplankton in deep-sea cores from the Caribbean Sea. Palaeontology, v.10, no.1, p.95-123, pl.14-16.

OPERCULODINIUM - Wall, D., 1967: Fossil microplankton in deep-sea cores from the Caribbean Sea. Palaeontology, v.10, no.1, p.95-123, pl.14-16.

PALAEOCYSTODINIUM - Alberti, G., 1961: On the knowledge of mesozoic and tertiary dinoflagellates and hygroscopic phosphaerides of northern and central Germany as well as some other European regions. Palaeontographica, Division A, v.116, p.1-58, pl.1-2.

PALAEOPERIDINIUM - Deflandre, G., 1934: On microfossils of planktonic origin, preserved in the state of organic matter in flints of chalk. Weekly reports of the sessions of the Academy of Sciences, v.199, p.966-968.

RHOMBODINIUM - Gocht, H., 1955: Rhombodinium and Dracodinium, two new dinoflagellates from the northern German Tertiary. New Year's Book for Geology and Paleontology, Monatshefte, no.2, p.84-92.

ROTTNESTIA - Cookson, I.C. and Eisenack, A., 1961b: Tertiary microplankton from the Rottnest Island Bore, Western Australia. Journal of the Royal Society of Western Australia, v.44, p.39-47, pl.1-2.

SPINIFERITES - Mantell, G.A., 1850: A Pictorial Atlas of Fossil Remains Consisting of Coloured Illustrations Selected from Parkinson's "Organic Remains of a Former World", and Artis's "Antediluvian Phytology". xii+207 p., 74 pl.; Henry G. Bohn, London, U.K.

WETZELIELLA - Lentin, J.K. and Williams, G.L., 1976: A monograph of fossil peridinioid dinoflagellate cysts. Bedford Institute of Oceanography, Report Series, no.BI-R-75-16, 237 p. [Cover date 1975, issue date 1976]